JOURNAL OF QUATERNARY SCIENCE (2005) **20**(2) 113–133

Published online in Wiley InterScience (www.interscience.wiley.com). DOI: 10.1002/jqs.902

Marginal formation of De Geer moraines and their implications to the dynamics of grounding-line recession

MATTIAS LINDÉN* and PER MÖLLER
GeoBiosphere Science Centre, Quaternary Sciences, Lund University, Sölvegatan 12, SE 22362 Lund, Sweden

Lindén, M. and Möller, P. 2005. Marginal formation of De Geer moraines and their implications to the dynamics of grounding-line recession. *J. Quaternary Sci.*, **Vol. 20** pp. 113–133. ISSN 0267-8179.

Received 16 April 2004; Revised 11 November 2004; Accepted 20 November 2004

ABSTRACT: De Geer moraine ridges occur in abundance in the coastal zone of northern Sweden, preferentially in areas with proglacial water depths in excess of 150 m at deglaciation. From detailed sedimentological and structural investigations in machine-dug trenches across De Geer ridges it is concluded that the moraines formed due to subglacial sediment advection to the ice margin during temporary halts in grounding-line retreat, forming gradually thickening sediment wedges. The proximal part of the moraines were built up in submarginal position as stacked sequences of deforming bed diamictons, intercalated with glaciofluvial canal-infill sediments, whereas the distal parts were built up from the grounding line by prograding sediment gravity-flow deposits, distally interfingering with glaciolacustrine sediments. The rapid grounding-line retreat (ca. 400 m yr^{-1}) was driven by rapid calving, in turn enhanced by fast iceflow and marginal thinning of ice due to deforming bed conditions. The spatial distribution of the moraine ridges indicates stepwise retreat of the grounding line. It is suggested that this is due to slab and flake calving of the ice cliff above the waterline, forming a gradually widening subaqueous ice ledge which eventually breaks off to a new grounding line, followed by regained sediment delivery and ridge build-up. Copyright © 2005 John Wiley & Sons, Ltd.

KEYWORDS: De Geer moraines; glacial sedimentology; subaqueous deglaciation; grounding line; deforming bed.

Introduction

Rapid decay of the last Scandinavian Ice Sheet succeeded the Younger Dryas cold-event readvance from the Skövde-Billingen Moraines in Sweden (e.g. Lundqvist and Wohlfarth, 2001; Fig. 1a) and the Salpausselkä Moraines in Finland (e.g. Donner, 1995; Fig. 1a). Along a flow-line from the Salpausselkä Moraines towards the last ice remnants in northern Sweden, the ice margin retreated 800 km within ca. 2000 years, between 11 500 and 9500 cal. yr BP, equal to a mean recession rate of ca. 400 m yr^{-1}. Climate probably provided a strongly negative mass balance on the ice sheet driving this rapid deglaciation (Siegert and Dowdeswell, 2002). Glacier dynamics and the deglacial environment were also important factors; longitudinal ice-sheet lineation patterns north of the Younger Dryas Moraines indicate the existence of major ice streams over Finland and the Gulf of Bothnia during ice-sheet decay (Boulton *et al.*, 2001b), enhancing the evacuation of large ice masses, and the ice margin was situated in deep water (up to ca. 330 m in the deepest part of the Gulf of Bothnia), promoting a retreat dominantly forced by calving. It is unknown, however, whether climate or glacier physics was the main trigger behind this rapid decay of the large ice volume.

The rapid deglaciation of coastal Norrbotten, northern Sweden (Fig. 1), left vast areas of recessional landforms such as *De Geer moraines* and *Niemisel moraines*. Our ongoing research project has a special focus on the formation of these landforms, with the main aim of reconstructing the sedimentological and landforming processes, and from this deducing the deglaciation pattern and dynamics of the area. The emphasis in this paper will be on De Geer moraines (Hoppe, 1959; in North America usually named washboard or cross-valley moraines, e.g. Mawdsley, 1936; Norman, 1938; Elson, 1957; Andrews, 1963a, 1963b; Prest, 1968), a type of moraine often abundant in areas characterised by subaqueous deglaciation. This work aims to demonstrate that De Geer moraines are strictly ice-marginal features and, as such, significant archives for our understanding of sedimentary grounding-line processes. They thus have bearing on grounding-line and calving dynamics and help us to understand rapid ice-sheet decay. Our interpretations are based on detailed sedimentological and structural investigations of De Geer moraines, combined with geomorphologic expression and spatial distribution patterns, and form the basis for a process/facies model of De Geer moraine formation in Norrbotten. Hopefully, this model also will have a bearing on the formation of similar moraine ridges elsewhere.

* Correspondence to: M. Lindén, GeoBiosphere Science Centre, Quaternary Sciences, Lund University, Sölvegatan 12, SE 22362 Lund, Sweden.
E-mail: mattias.linden@geol.lu.se

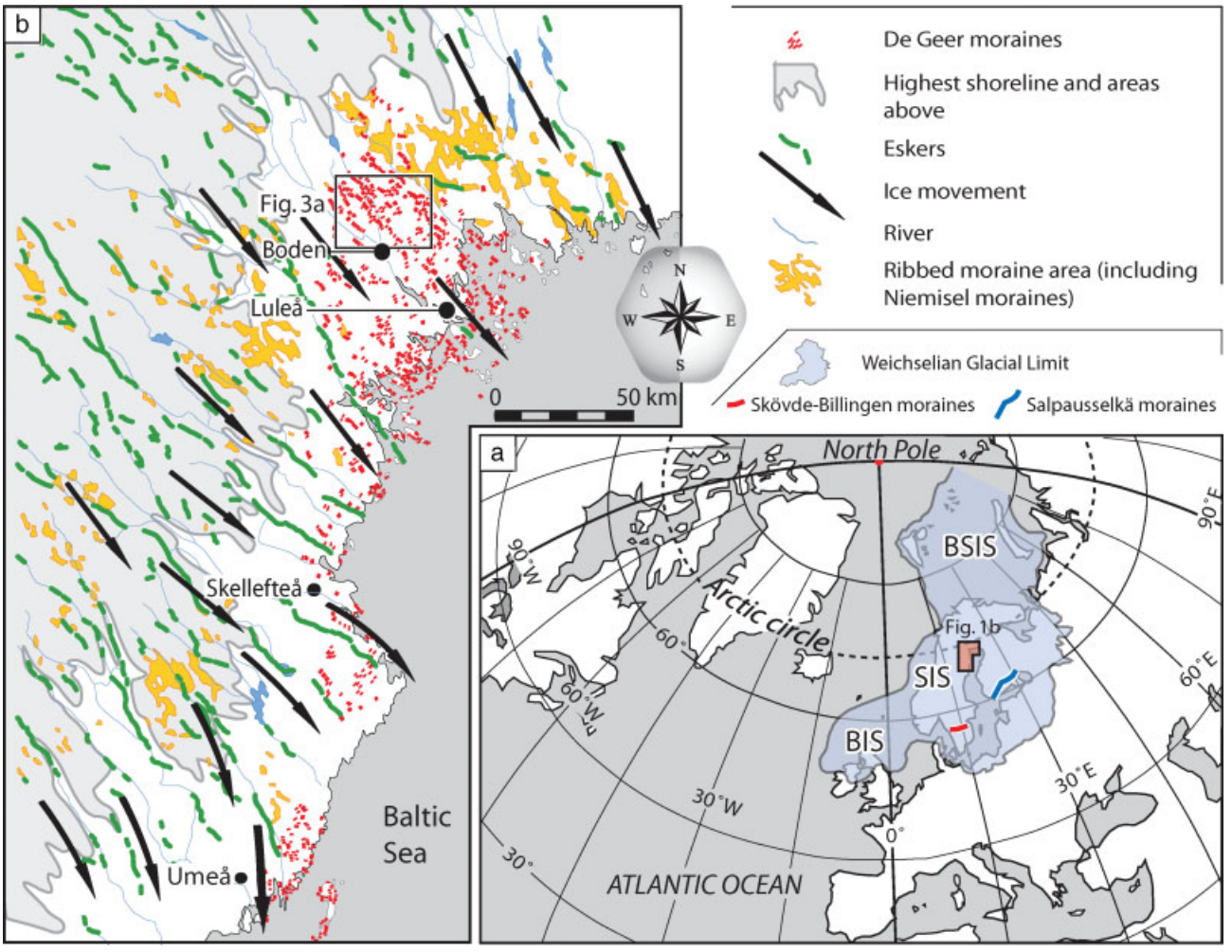

Figure 1 a. Overview map showing coastal Norrbotten in relation to the Late Weichselian glaciation maximum over Fennoscandia. Ice Sheet boundaries according to Svendesen *et al.* (1999). BIS = British Ice Sheet; SIS = Scandinavian Ice Sheet; BSIS = Barents Sea Ice Sheet. b. Spatial distribution of glacial landforms and last iceflow directions along the coast of Norrbotten, northern Sweden (modified from Hättestrand, 1997). The position of the highest coastline is from Lundqvist (1994). The location of Fig. 3a is indicated

De Geer moraines—previous work

De Geer moraines are abundant in areas below the highest shoreline/marine limit in Scandinavia, forming swarms of small moraine ridges roughly transverse to the former iceflow direction. Ridges of this type were described as early as 1889 by Gerhard De Geer. From the area around Stockholm, sets of small-scale moraine ridges were interpreted as annual moraines (in Swedish, 'årsmoräner'), suggested to be dump moraines deposited at a water-terminating ice margin during winter stillstands. The formative processes were later suggested to be pushing and stacking of sediments, i.e. push moraines, at the ice margin during winter readvances of a generally retreating ice sheet (De Geer, 1940). De Geer also argued that the concept of annual formation of the moraine ridges was supported by his varve chronology as the average distance between adjacent ridges usually coincides with the ice recession rate in central parts of Sweden, based on varve counting.

De Geer moraines have drawn considerable attention, resulting in a large number of investigations aimed at revealing their depositional history. In spite of this, the active processes responsible for sediment formation and landform generation seem to be poorly understood. Most of the earlier investigations (e.g. De Geer, 1889; Hoppe, 1948, 1957, 1959; Möller, 1962; Lundqvist, 1989; Strömberg, 1965; Zilliacus, 1985, 1987, 1989) on De Geer moraines are based on geomorphology, spatial distribution patterns and ice-sheet recession chronology (varves), and only to a limited extent on sedimentological and structural evidence. However, attention has shifted towards sedimentological investigations in an attempt to reveal the processes responsible for De Geer moraine formation (Sollid and Carlsson, 1984; Beaudry and Prichonnet, 1991, 1995; Larsen *et al.*, 1991; Blake, 2000).

Hoppe (1948) argued, based on field evidence from Norrbotten, that more than one moraine ridge (ca. 2–3) was formed every year. This was calculated from the relation between the mean distance between moraine ridges and the mean annual ice-retreat rate, obtained from varve chronology (De Geer, 1940). Hoppe (1959) proposed an alternative hypothesis on moraine ridge formation which included the seasonal velocity variations of active glaciers; as no evidence of winter stillstands or readvances were identified, moraine ridge formation was suggested to occur during the warmer seasons when the velocity of the ice sheet was at its maximum. Hoppe (1959) suggested that squeezing was the main process of transferring sediments to the ice front and into submarginal crevasses parallel to the ice margin, and that usually more than one ridge was produced during each melt season. It was concluded, when interpreting the 'annual' moraines as not being annual, that the term annual moraines was misleading and he therefore renamed them De Geer moraines after their first describer (Hoppe, 1959).

Strömberg (1965) agreed with Hoppe's (1959) hypothesis of sediment squeeze into submarginal crevasses, on the basis of

his observations in the Uppsala area in Sweden. Zilliacus (1985, 1987, 1989) investigated De Geer moraines in Finland, and he also suggested formation by subglacial squeeze into crevasses, although into sets of basal transverse crevasses initiated by glacial surges. This view has also been supported by Lundqvist (1989, 2000). The ice-surge hypothesis by Zilliacus does not, however, take into account—or explain—the classical calving bay configuration seen in many De Geer moraine areas (Strömberg, 1981, 1989).

Based on sedimentological investigations on De Geer moraines in the Möre and Pasvik areas, western and northern Norway, respectively, Larsen *et al.* (1991) and Sollid and Carlsson (1984) concluded that the ridges were deposited as annual recessional moraines at the ice margin. Sollid and Carlsson (1984) argued that formation was by lodgement of basal debris at the margin during the winter season. Furthermore, they dismissed formation of basal crevasses since the plastic behaviour of the ice would prevent the development of such crevasses. It was also proposed that the similarity in basal stress and hydrostatic pressure between the basal water and the water in the adjacent basin (no effective stress gradient) would prevent marginal squeeze of saturated till. Larsen *et al.* (1991) suggested stacking of sediments by pushing at the grounding line, and that the retreat was mainly controlled by iceberg calving. They rejected the crevasse model, since preservation would require an ice lift-off over a wide area and considered this mechanism highly unlikely because the glacier outlets were strongly controlled by the fjord topography.

Based on extensive sedimentological investigations on De Geer moraines from Québec, Canada, Beaudry and Prichonnet (1991, 1995) concluded that these were formed due to basal crevasse infill beneath an active glacier. In areas with abundant basal meltwater canals, prograding beds of sorted material were suggested to accumulate in crevasses by foreset migration, whereas infill of till should be the case in areas where meltwater flow was absent. Subglacial shear was suggested to remobilise basal till locally and push it in a down-glacier direction into basal crevasses and also overturn thick till beds, previously deposited in these crevasses. Their proposed model for De Geer moraine formation implies that a number of moraines can be formed simultaneously inside the grounding line and, accordingly, that they are not annual features.

Blake (2000) investigated De Geer moraine formation from the Svartisen area, northern Norway, and reached the conclusion that ridges formed at the grounding line were mainly composed of sorted sediments and basal till. It was argued that the stratigraphy indicated periods of deposition of sorted sediments, followed by periods of till deposition and deformation of pre-deposited sediments. According to Blake (2000) the number of till units, separated by sorted sediment beds in a single moraine ridge, could indicate the number of times the grounding line reoccupied the specific position, thus discrediting the annual moraine hypothesis.

Geological setting of the investigation area—regional introduction

Regional geomorphology

The large-scale geomorphology of the investigation area is characterised by southeast-trending broad valleys and bedrock hills, the latter reaching altitudes of 600 m a.s.l. (Fig. 1). Streamlined bedrock knobs, drumlins and lee-side moraines, all preferentially on higher ground, indicate a predominating ice movement towards the southeast, possibly repeated through several glacial cycles (Fromm, 1965; Lundqvist, 1981; Hättestrand, 1997; Kleman, 1990, 1992; Kleman *et al.*, 1997).

Valleys are predominantly occupied by till and glaciolacustrine/lacustrine silt, while glaciofluvial sediments seem to have a very restricted occurrence. Often the thickness of glaciolacustrine deposits increases towards the present coast as the valleys become wider. Most of the till below the highest shoreline is represented by the local 'Kalixpinnmo' till, most typically seen as bimodal, poorly sorted sediment predominated by fine sand with dispersed coarse clasts (Beskow, 1935; Fromm, 1965; Hoppe, 1948, 1952, 1959; Lundqvist, 1981). Till surfaces are significantly wave-washed below the highest shoreline (200–220 m a.s.l.) and beach sediments frequently occur just below the highest shoreline and on slopes exposed to wave action during regression.

Morainic landforms are abundant in low-lying terrain, especially De Geer moraines, but also large, continuous areas of Niemisel moraines (Hoppe, 1948; Fromm, 1965; for areal distribution see SGU Ak map series: Gråsäs, 1990; Svedlund, 1991, 1992; Rodhe and Svedlund, 1990). De Geer and Niemisel moraines are usually spatially separated, but in some areas these moraines occur together and De Geer moraines are at several places seen to be superimposed on Niemisel moraines.

Spatial distribution of De Geer moraines

De Geer moraines are found below the highest shoreline of the last glacial event and extend well below the present sea level in the Gulf of Bothnia. Thus De Geer moraines are abundant in a 30–100 km wide zone along the coast of Norrbotten (Fig. 1). In general, the height of De Geer moraines in Norrbotten varies between 1 and 3 m, although heights up to 6–7 m have been recorded (Hoppe, 1948; Fromm, 1965). The average width is ca. 30 m and the length is highly variable; some ridges are only 100 m long while others can be traced continuously over distances of 2–3 km. The cross-sectional shape varies, but most commonly shows a gently sloping proximal side and a somewhat steeper distal side (Fig. 2). The typical morphology is therefore a rather low, narrow and elongated moraine ridge with variable length. The distance between adjacent ridges is usually between 50 and 200 m, occasionally up to 500 m. However, the average distance is ca. 100–150 m.

With respect to iceflow direction De Geer moraine tracts form a transverse lineation pattern being slightly upflow concave in valleys and topographic lows and slightly convex over, or close to, elevated ground (Fig. 3a). This refers to the large-scale trend of De Geer moraines, even though individual ridges may diverge from this pattern. Occasionally two or three De Geer moraines converge towards the valley side or when approaching topographic heights. Though rare, this feature is more frequent for smaller (i.e. <1 m high) moraine ridges. Even though the frequency of De Geer moraines is smaller on higher ground and close to the highest shoreline, they are often found on lower topographic heights and half-way up on valley sides. In these positions the moraine ridges are often small and flat. The rarity of moraine ridges on the heights might be due to wave-washing during the isostatic uplift, which at places is supported by linear occurrences of residual boulders, but also might be because the ridge-forming processes were unfavourable in this position.

De Geer moraines are sometimes not recognised in the central parts of the valleys. However, this is most probably a 'masking' effect as lakes, rivers, mires and fine-grained sediments frequently occupy or cover the valley floor. Small moraines

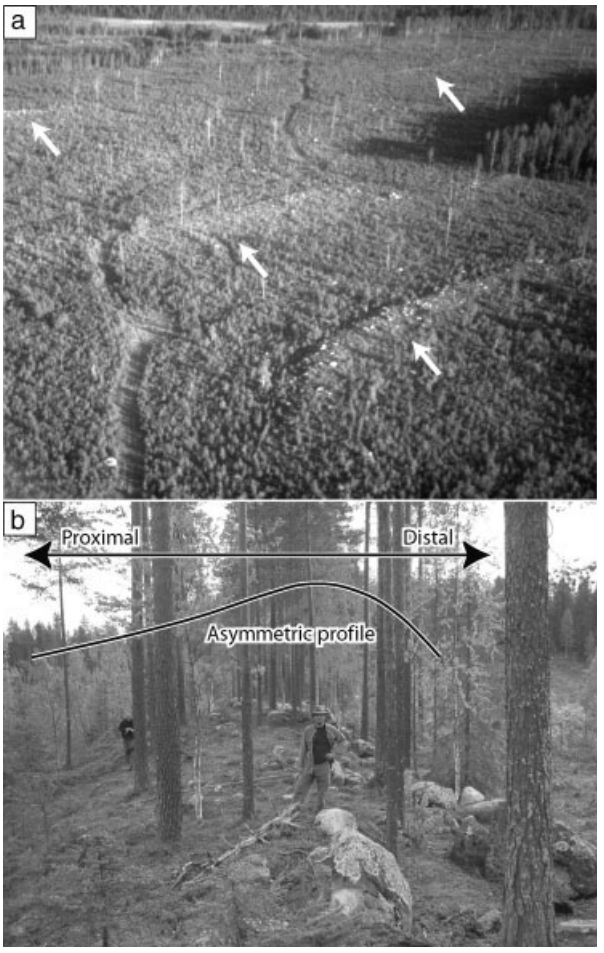

Figure 2 a. Oblique aerial photograph showing three narrow and slightly curved De Geer moraines marked by arrows, also indicating the iceflow direction. b. Typical De Geer moraine with asymmetric cross profile and boulder concentration. Iceflow was from left to right

in mid-valley position are probably especially vulnerable to being buried by fine-grained sediments; this might explain locally large distances between moraine ridges. Natural breaks in the terrain, such as, for example, thresholds for lakes, often indirectly indicate De Geer moraine location on valley floors.

Deglaciation of the area—present knowledge

The accepted concept for northern Sweden is that, prior to deglaciation, the ice divide moved from the Bothnian basin to the mountain region, from east to west (Lundqvist, 1994). The freshwater Ancylus Lake (Björck, 1995) gradually inundated the area as the ice margin retreated westwards and most of the investigated area was below sea level at deglaciation. However, the most elevated parts of the terrain formed an archipelago at the time of deglaciation with islands and peninsulas along which the highest shoreline was developed at ca. 200–220 m a.s.l. (SGU Ak map series: Grånäs, 1990; Svedlund, 1991, 1992; Rodhe and Svedlund, 1990). The highest shoreline is well developed on the higher bedrock knobs, sometimes resulting in formation of till-capped hills. The altitude of the highest shoreline decreases from the present coast and further inland due to higher isostatic uplift within the Gulf of Bothnia, where the ice sheet was at its thickest during the maximum glaciation (Lundqvist, 1994). A secondary cause is that the landscape had already begun to rise faster than sea-level rise when the ice margin retreated across the area, gradually exposing new areas to the Gulf of Bothnia and subsequent wave action. Hence, during this inundation of Norrbotten by Ancylus Lake the regressive and asynchronous highest shoreline was formed. Isostatic uplift is a still-continuing process in the coastal areas of Norrbotten, raising the land at present by slightly less than 1 cm yr^{-1} (Eriksson and Henkel, 1994). The area was deglaciated approximately at ca. 10 000 cal. yr BP according to Lundqvist (1994) and varve-chronology data suggest that the ice retreat rate was approximately 300–400 m yr^{-1} in Norrbotten (De Geer, 1940) and 300–500 m yr^{-1} in Västerbotten (Bergström, 1968).

Methods

Morphological mapping of moraines was conducted by means of aerial photographic interpretation. Most of the aerial photographs used were black and white photographs at a 1:30 000 scale. If available, false-coloured infrared photographs (1:60 000 scale) were also used in order to cover larger areas. The mapping was done partly as a supplement to the sediment/landform maps at a scale of 1:50 000, published by the Swedish Geological Survey (Grånäs, 1990; Svedlund, 1991, 1992; Rodhe and Svedlund, 1990) and to construct high-resolution maps of the area with a higher control of distribution and spacing of the moraine ridges.

Digital topographic data was put at our disposal by the Swedish Geological Survey to produce Digital Elevation Models (DEMs). ArcView served as a platform from which basic map calculations were performed and a map of the highest shoreline was generated. The digital data was also manipulated for shadowing (sun angle) effects in order to highlight minor topographic lineations, which sometimes proved useful in connection with the aerial photographic interpretation.

Sedimentological investigations were carried out in excavated trenches, perpendicular to the ridge crests. Lithologic units were recognised on the basis of lithofacies classification (Table 1). The boundaries between lithofacies units, their internal structures and deformation structures, were measured and documented at a scale of 1:20. Sediment samples were taken for grain size analysis.

Clast fabric analyses were carried out on prolate pebbles, excavated from 50 × 30 cm horizontal benches in the sections and with vertical sampling less than 20 cm. Each fabric set comprises 30 pebbles with the longest axis (*a*-axis) ranging between 2 and 12 cm, and only clasts with an *a*/*b*-axis ratio of ≥ 2 were accepted. Pebbles with close contacts to boulders and other pebbles were discarded because of possible orientation interference. The orientation data were statistically evaluated according to the eigenvalue method of Mark (1973) and graphically manipulated with StereoNet© 1.01 for Windows.

Ljuså and Rasmyran, type areas for sedimentological investigations of De Geer moraines

The area around Boden shows a high concentration of De Geer moraines (Fig. 3a). Two type-areas were chosen for more detailed investigations, the Ljuså area (Fig. 3b) situated 18 km north of Boden and the Rasmyran area (Fig. 3c) situated 12 km west of Boden. The numerous De Geer moraines in the area around Ljuså show with respect to palaeo-iceflow direction a slightly concave/convex plan-form distribution pattern. The

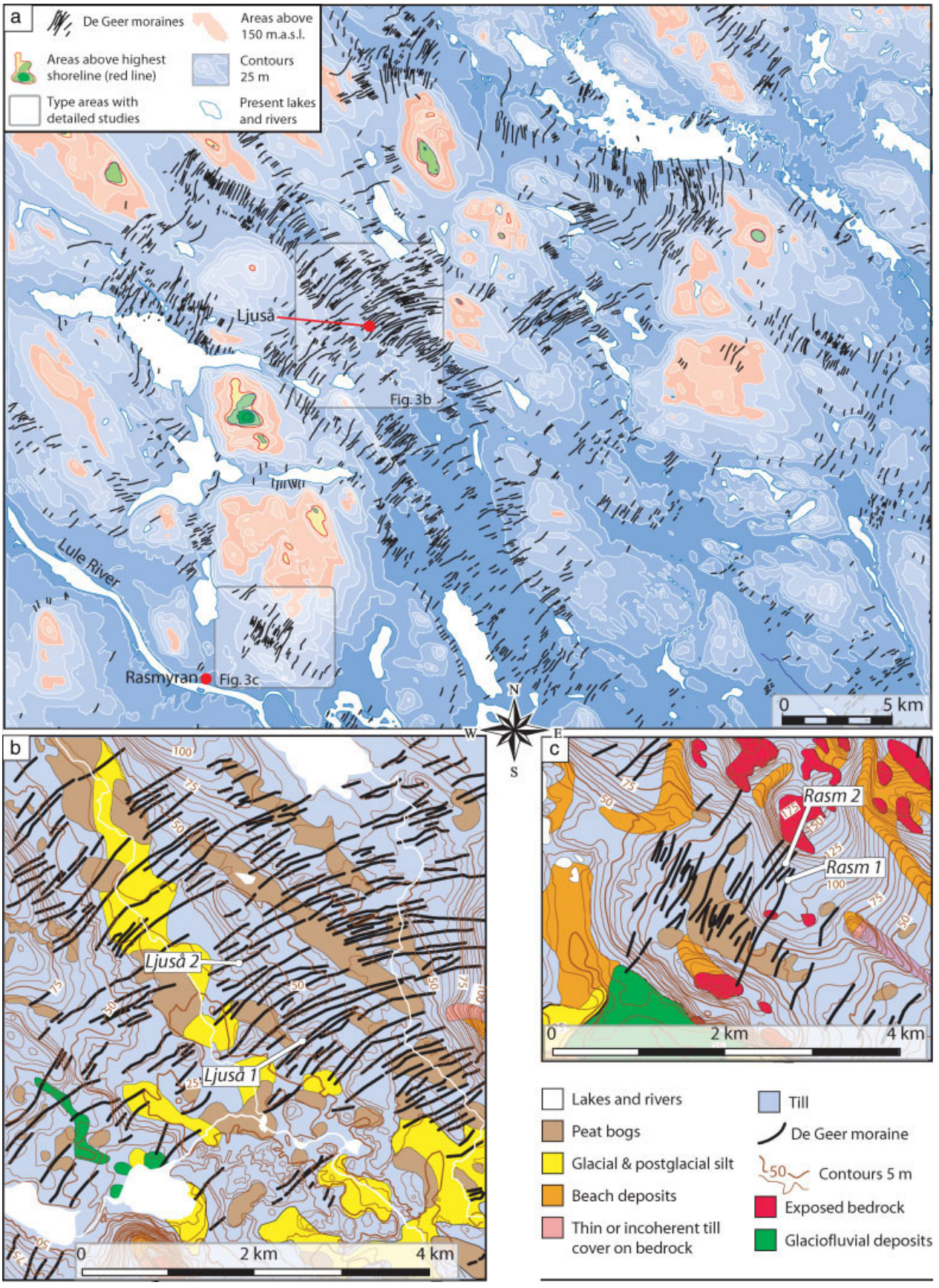

Figure 3 a. Spatial distribution of De Geer moraines, compiled from SGU Ak-series maps (Grånäs, 1990; Svedlund, 1991, 1992; Rodhe and Svedlund, 1990) and aerial photographic interpretation. The bathymetry at deglaciation is indicated, as well as the highest shoreline at 210–220 m a.s.l. Inserts mark the position of Figs 3b and 3c. The city of Boden is situated below 'S' in compass rose. b. Detailed spatial distribution of De Geer moraines and sediments in the Ljusa area, based on map by Grånäs (1990). Positions of excavated De Geer moraines are indicated. c. Detailed spatial distribution of De Geer moraines and sediments in the Rasmyran area, based on map by Rodhe and Svedlund (1990). Positions of excavated De Geer moraines are indicated

Table 1 Lithofacies codes (first-, second- and third-order code system) and their descriptions as used in this work (basic system according to Eyles *et al.*, 1983)

Lithofacies code	Lithofacies type description: grain size, grain support system, internal structures
D(G/S/Si/C)	Diamicton, gravelly, sandy, silty or clayey. One or more grain-size code letters within brackets
D( )mm	Diamicton, matrix-supported, massive
D( )ms	Diamicton, matrix-supported, stratified
Co–	Cobbles, as below
D( )mm(ng)	Diamicton, matrix-supported, massive, normally graded
D( )mm(ig)	Diamicton, matrix-supported, massive, inversely graded
D( )mm (ing)	Diamicton, matrix-supported, massive, inverse to normally graded
Gmm	Gravel, matrix-supported, massive
Gcm	Gravel, clast-supported, massive
Gc(ng)	Gravel, clast-supported, normally graded
Gc(ig)	Gravel, clast-supported, inversely graded
Sm	Sand, massive
Sm(ng)	Sand, massive, normally graded
Sm(ig)	Sand, inversely graded
Spp	Sand, planar parallel-laminated
Spc	Sand, planar cross-laminated
Stc	Sand, trough cross-laminated
Sr	Sand, ripple-laminated
Sl(def)	Sand, laminated, deformed
Sim	Silt, massive
Sil	Silt, laminated

ridges have an up-glacier concave outline in low-lying areas of the valley and tend to curve down-glacier when approaching higher terrain. Conversely, the De Geer moraines in the area around Rasmyran show a straighter distribution pattern transverse to the valley, and the palaeo-iceflow direction, and show no significant trend to curve in any direction. These ridges are situated closer to the highest shoreline (ca. 100–120 m water depth at deglaciation) and exposed bedrock, thin till cover and beach deposits are more frequent (Fig. 3c), suggesting a higher degree of exposure to wave action than in the Ljuså area (ca. 160–180 m water depth at deglaciation). In each type area two moraines were chosen for sedimentological investigations in machine-dug trenches. Those chosen for the Ljuså area are situated in a densely packed ridge area; between Ljuså 1 and Ljuså 2 (Fig. 3b) there are 13 individual moraines, which give an average of 90 m between ridge crests. The moraines chosen in the Rasmyran area are just ca. 200 m apart (Fig. 3c), with a short ridge in between. The trenches were 28 to 37 m long, covering the whole or most of the cross-sectional area of each ridge, and the excavation depths (4–5 m) extended beneath the morphological expression of the ridges.

Sediments—descriptions and interpretations

All four trenches crossing the De Geer moraine ridges reveal a similar large-scale sedimentary and deformational architecture and can therefore be described together as a general framework for facies variability within and in connection to the moraines. Seven sedimentary facies are recognised along the studied section walls. Facies 1–4 are the primary building components in context of De Geer moraine formation, whereas facies 5–7 interfinger, overlie or onlap without being primary constructional sediment bodies of the moraine ridges. The formative facies (1–4) are represented by sandy-silty diamicton (facies 1) and gravelly-sandy diamicton (facies 2), the former predominantly located on the proximal side and the latter on the distal side of the moraines, and predominantly massive to laminated sand and silt (facies 3) interbedded with the diamict facies. Facies 4 is sand and gravel, forming injection structures on the proximal side of the moraines.

Facies descriptions, facies 1–4

Facies 1, sandy-silty diamicton. This facies is the predominant facies in all four De Geer moraine sections, represented by a grey, sandy-silty, matrix-supported and massive diamicton (D(SSi)mm; see Table 1 for lithofacies codes). This sandy-silty diamicton constitutes the base of the landform and probably also forms the local till cover in both type areas. It predominates in the proximal parts of the ridges, but pinches out and usually interfingers with facies 2 diamicton distal to the ridge crest-lines. Facies 1 diamicton also occurs as isolated bodies (up to 2 m long and 0.5 m thick) within the facies 2 sandy-gravelly diamicton.

Although massive in structure, local variations in matrix texture are common with diffuse changes into a silty-sandy matrix, forming indistinct bodies of slightly more coarse-grained diamicton on a decimetre to metre scale. The clast content is high with randomly distributed subrounded to subangular cobbles and boulders, the maximum sizes being 1.2–2.5 m. Bedding planes in the massive diamicton are inferred from contacts to inter/intrabedded sediments of facies 3 (sand and silt). From this it can be deduced that the facies 1 diamicton—at least in the Ljuså 1, Ljuså 2 and Rasmyran 1 sections—constitutes sets of stacked beds, 0.5–4 m thick, with a primary up-glacier dip (6–35 °) with increasing inclination towards the crest-line. The intrabeds within the massive diamicton also reveal abundant dislocations, faulting and folding, comprising single beds or composite bed-sets, indicating series of syndepositional deformational events.

Seventeen fabric analyses were carried out in facies 1 diamictons at the different sites (Fig. 5), preferentially where visual indications of post-depositional disturbances were absent. Eleven analyses showed unimodal and clustered clast axis orientations with strength values (S_1) varying between 0.76 and 0.85, giving fabric shapes characterised by very low isotropy ($I = 0.011$–0.118) and very high elongation ($E = 0.654$–0.884; Fig. 6). Mean axis orientations (V_1) are perpendicular or slightly oblique to the local trend of moraine ridge crest-lines. The mean deflection of V_1 from being perpendicular to ridge crest-lines is 14.5 ° with a maximum deflection of 33 °. The remaining six fabric analyses revealed a distinctively different fabric shape (Fig. 6); five show girdle distributions of clast axes (Ljuså 2:2, 2:3 and Rasmyran 1:1, 1:2, 2:4; Fig. 5) with low (0.51–0.62) but, for girdle distributions, significant S_1 values. The dips of the distribution planes of three of these girdle distributions plunge near-parallel to ridge crest-lines, whereas two plunge near-to perpendicular and up-glacier to ridge crest-lines. The remaining fabric analysis, Rasmyran 2:3, shows a random clast-axis distribution with a number of clast axes with high angles of plunge. The biggest clasts, i.e. cobbles and boulders, showed no apparent preferred orientation, possibly with the exception of section Rasmyran 2 where a weak clustering, parallel to the overall iceflow direction, occurred.

Facies 2, gravelly-sandy diamicton. Facies 2 is a brown, gravelly-sandy to sandy-gravelly, massive and predominantly matrix-supported diamicton (D(GS)mm). This facies is restricted to the central and/or distal parts of all De Geer moraine sections, and pinches out and interfingers with facies 5 sediments in the distal direction (Fig. 4). Facies 2 is thus

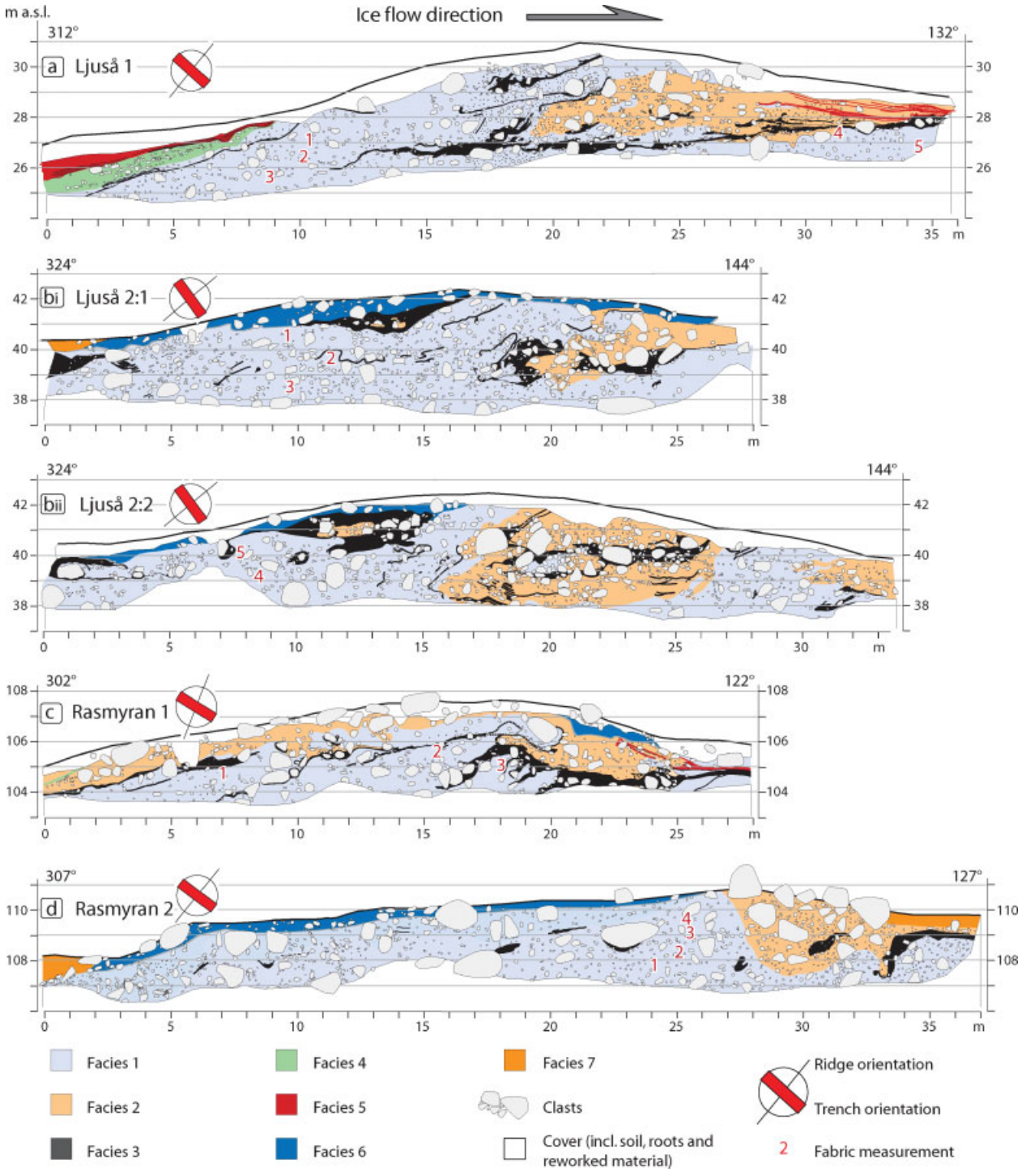

Figure 4 Profiles showing discerned sediment facies (see text for explanation) from the four excavated De Geer moraines. Iceflow direction from left to right. a. Section *Ljuså 1* (N 65 ° 58.147′; E 21 ° 38.039′). The most geomorphologically distinct of the excavated moraines, 300 m long, 30 m wide with a crest-line height above adjacent troughs of 5.0 m on its proximal side and 2.2 m on its distal side. b. Section *Ljuså 2* (N 65 ° 58.590′; E 21 ° 37.368′). This ridge is 300 m long and 38 m wide, and has a crest-line height above adjacent troughs of 3.2 m on its proximal side and 2.0 m on its distal side. Both trench walls were documented ($4b_i$ and $4b_{ii}$). c. Section *Rasmyran 1* (N 65 ° 52.394′; E 21 ° 31.741′). Geomorphologically a very distinct ridge which with only short breaks can be followed for nearly 1.5 km. At the excavation site it is ca. 40 m wide, and has a crest-line height above adjacent troughs of 3.4 m on its proximal side and 2.4 m on its distal side. d. Section *Rasmyran 2* (N 65 ° 52.489′; E 21 ° 31.671′). This ridge, ca. 250 m long, is situated in a pronounced upslope position with respect to palaeo-iceflow direction. At the excavated site the ridge is 32 m wide, but gives a very small geomorphological imprint, being just 0.8 m high on its distal side and 2.7 m high on the proximal side. The latter shows a step-like profile, enhanced with boulder concentrations continuing into surficial beach gravels

predominantly connected to the distal slope of the De Geer moraine ridges.

The diamicton is massive, but small-scale variations in sand/gravel ratios are common, in both the lateral and the vertical direction. Locally the diamicton grades into a nearly clast-supported state owing to very low matrix frequencies and thus high concentrations of larger clasts. In Ljuså 2 the facies 2 diamicton locally also grades into sorted coarse gravels with an open framework. The cobble and boulder content of facies 2 is slightly higher than that of facies 1, consisting of randomly distributed, subrounded to subangular cobbles and boulders, with maximum sizes of 1–2 m. In section Ljuså 1, the upper

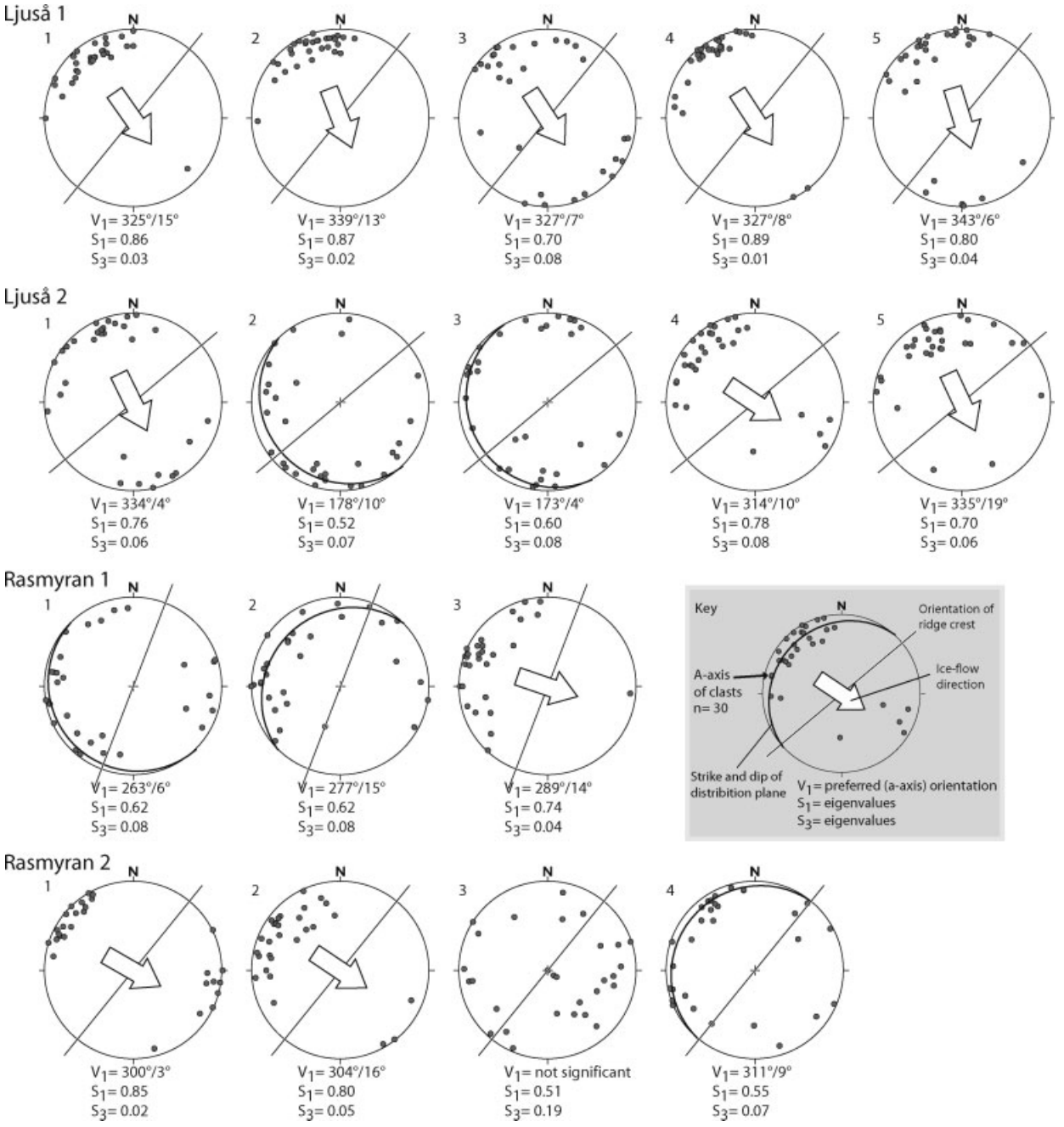

Figure 5 Schmidt equal-area, lower-hemisphere projections of clast long-axis orientations from fabric analyses (30 clasts measured in each set) at the four investigated sections (for positions within sections, see Fig. 4). Each scatterplot is accompanied by calculated largest eigenvector (V_1) and normalised eigenvalues (S_1 and S_3) according to Mark (1973). Inferred iceflow directions (arrows) are shown on fabric sets showing a high fabric strength value (S_1). For fabric sets showing significant girdle orientations a best-fit plane through the plotted data is drawn as a great circle. Ridge axis orientation is indicated in each plot

distal part of the gravelly-sandy diamicton is gradually replaced by a more fine-grained, sandy diamicton in the distal direction.

Bedding planes in the facies 2 diamicton are inferred from contacts to interbeds of facies 1 diamicton and facies 3 and 5 (sands and silts). These contacts are generally sharp, but locally gradational contacts are found. When not deformed, facies 2 beds have low-angle dips in the distal direction from the ridge crest-lines. As facies 2 occur in all section walls in a central to distal position it is concluded that this facies forms wedge-shaped sediment bodies distal to the ridge crest-lines.

From visual examination it was obvious that facies 2 diamicton has disturbed fabric orientations, for example due to frequent clast contacts, but especially caused by extensive post-depositional deformation of packages of facies 2 diamicton and facies 3 sorted sediments.

Facies 3, silt, sand and gravel. Facies 3 is an association of sorted sediments occurring as intrabeds within facies 1 and facies 3 diamictons. The facies is dominated by laminated to massive fine sand and silt, but also beds of usually massive (sometimes normally graded) sand, gravelly sand and gravel are common. Out-sized clasts occur frequently, also in the silt and fine sand facies; smaller clasts (1–2 cm) are common and clasts up to 15–30 cm in diameter are not uncommon. Larger clasts in otherwise undeformed (see below) facies 3 silt and fine sand are sometimes associated with basal/lateral small-scale deformation structures. Occasionally very large clasts (60–120 cm) within facies 3 sediments protrude upwards into overlying unit 1 diamicton. These clasts should not be mistaken for those belonging to facies 1 diamicton, protruding down into facies 3 sediments and always associated with deformation structures.

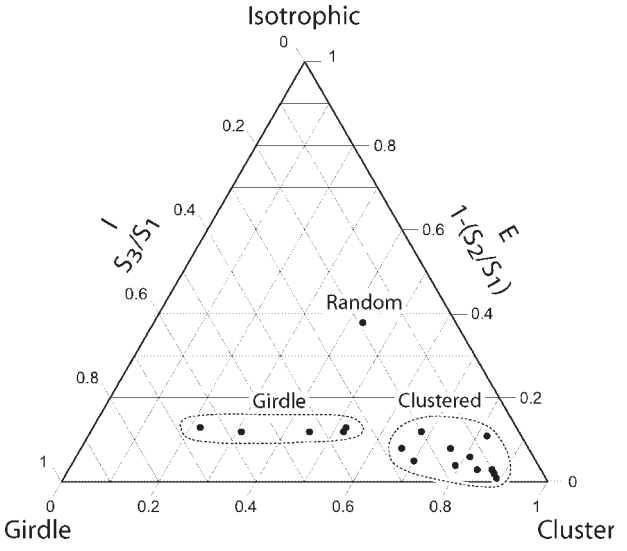

Figure 6 Fabric shape data—isotrophy index (I; $I = S_3/S_1$) and elongation index (E; $E = 1 - S_2/S_1$) plotted in a triangular diagram (Benn, 1994). Most *a*-axis fabric eigenvalue data of facies 1 diamicton indicate low isotropy and very high elongation of clast long-axis orientations

Facies 3 beds occur in all sections, both as thin (1–2 cm) solitary sets and as stacked, thicker (up to ca. 100 cm) cosets, and when not part of large-scale fold structures the beds are subhorizontal to gently inclined in the proximal direction. Their lateral continuity is highly variable (0.5–20 m) in different sections, the most continuous one being the lowest facies 3 bed in the Ljusåå 1 section (Fig. 4a), starting well behind the crest-line and continuing in the distal direction outside the morphological expression of the ridge. The lower contact of facies 3 beds is always sharp, whereas the upper contact sometimes is gradational or welded to the overlying diamicton. Facies 3 sediments are more frequent as intrabeds within the facies 1 sandy-silty diamicton than in the facies 2 diamicton, and often also form interbeds between facies 1 and 2 with draping but sharp lower contacts.

The beds occur both in their primary depositional position with primary sedimentary structures preserved (Fig. 7), and as deformed beds. Deformation structures are of different scales; some beds reveal intrabed folding and small-scale thrusting (one to a few centimetres) of internal lamination (Fig. 7d), with beds more or less in their primary position, whereas some deformations, as in the Ljusåå 1 and 2 sections, are of a larger scale (decimetre to metre scale) involving both facies 3 sorted sediment beds and enclosing facies 1 diamicton. These larger-scale structures include: up-thrusts of laminated facies 3 beds, standing at steep angles on the lee-sides of larger boulders (Fig. 7a, c); folding (upright, inclined and overturned folds) of single couplets or packages of facies 3 and 1 sediments (Fig. 4); more or less totally contorted facies 3 sediments (Fig. 7b) associated with intrusion of facies 1 diamicton and/or extrusions of facies 3 sediments into the diamicton. All large-scale folds and thrust structures within the section walls were mirrored at right-angles on the opposite section walls, suggesting fold axes parallel or subparallel to the ridge.

The Rasmyran 2 section differs from the other sections by facies 3 sediments being not common (Fig. 4d). However, in the distal part of this section a thick coset of facies 3 fine sand, sand and gravelly sand, located at the interface between facies 1 and facies 2 diamicton, is involved in a lateral compression of the whole sequence with highly inclined facies 3 sediment bedding (Fig. 8). The result of the compression is two large-scale fold structures with the facies 3 sediments conforming to the fold configuration (Fig. 4d). Measurements on fold limbs (Fig. 8) give a mean fold axis trend of 61–241 °, which is nearly parallel (deviation 22 °) to the crest-line trend of the ridge.

Facies 4, massive cobble gravel. Facies 4 constitutes a clast-supported, massive, cobble and boulder-rich, moderately sorted gravel (maximum clast size 40–50 cm and with a most-common large clast size of 10–15 cm). These sediments form an onlapping bed, being 70 cm in its thickest observed part on the proximal lower part of the Ljusåå 1 ridge (Fig. 4a). Facies 4 sediments are also present at the same position in the Rasmyran 1 section, but were not observed at Ljusåå 2 or Rasmyran 2. In the section wall opposite to the one documented in Ljusåå 1, three wedges of gravelly sand intrude downward from the base of the facies 4 gravel (here 10–15 cm thick, Fig. 7e) into the underlying facies 1 diamicton (clastic dykes, cf. Dionne and Shilts, 1974). They are 50–120 cm wide at their entrances into the diamicton, and up to 1.5 m deep and downward-tapering. The infilling sediment, coloured by secondary red-brown iron oxide precipitation which accentuates the boundaries with the enclosing diamicton, change gradually in grain-size from coarse gravel to gravelly sand and eventually to massive medium sand in the thin, slightly up-curving, distal end of the dykes. One small clastic dyke is also present in the section wall at Ljusåå 1. It emanates from the facies 4 sediment beds and plunges steeply into the below-lying sandy silty diamicton. When reaching a bed of fine sand and silt, it deflects in down-glacier direction and can be traced along this bed for a short distance.

Interpretations, facies 1–4

Based on its sediment characteristics, facies 1 (the sandy-silty diamicton) is interpreted as a deformation till (e.g. Benn and Evans, 1996). To achieve deforming bed conditions the induced shear stresses must reach or exceed the internal yield strength of the subglacial sediment. This requires high pore-water pressure in the substrate in order to reduce the effective stress, and concordantly the shear strength, enabling the bed to become mobile (Boulton, 1996). The massive structure implies a high strain rate during deformation. However, a total homogenisation of the deforming bed layers was not always reached, as indicated by the indistinct, small bodies of slightly more coarse-grained diamicton, resembling boudinage structures. The repetitive inter/intrabedding of facies 1 till beds and facies 3 sorted sediment beds implies that deforming bed conditions—and the 'freezing' of the bed movement—were fulfilled repetitively, forming a superimposed succession of deforming bed units, i.e. what has been termed constructional subglacial glaciotectonic deformation by Hart and Boulton (1991). These deforming layers were most probably thin, as expected in the marginal area of an ice sheet (e.g. Boulton and Hindmarsh, 1987; Hart and Boulton, 1991). This is directly indicated from till bed thicknesses but also indirectly from till fabric data. The unimodal and clustered clast axis orientations, all with high strength values ($S_1 = 0.70$–0.89; Fig. 5), are considered as being orientated parallel to the iceflow-induced stresses field, applied during deforming bed conditions. Such well-ordered orientation is suggested to be indicative of thin deforming-bed zones (e.g. Hart, 1994; Benn, 1995; Hart and Rose, 2001) undergoing ductile shear (Boulton and Hindmarsh, 1987; Benn and Evans, 1996). The five girdle-orientated and the randomly orientated fabric analyses are suggested to represent, with respect to deforming bed conditions, post-depositional reorientation

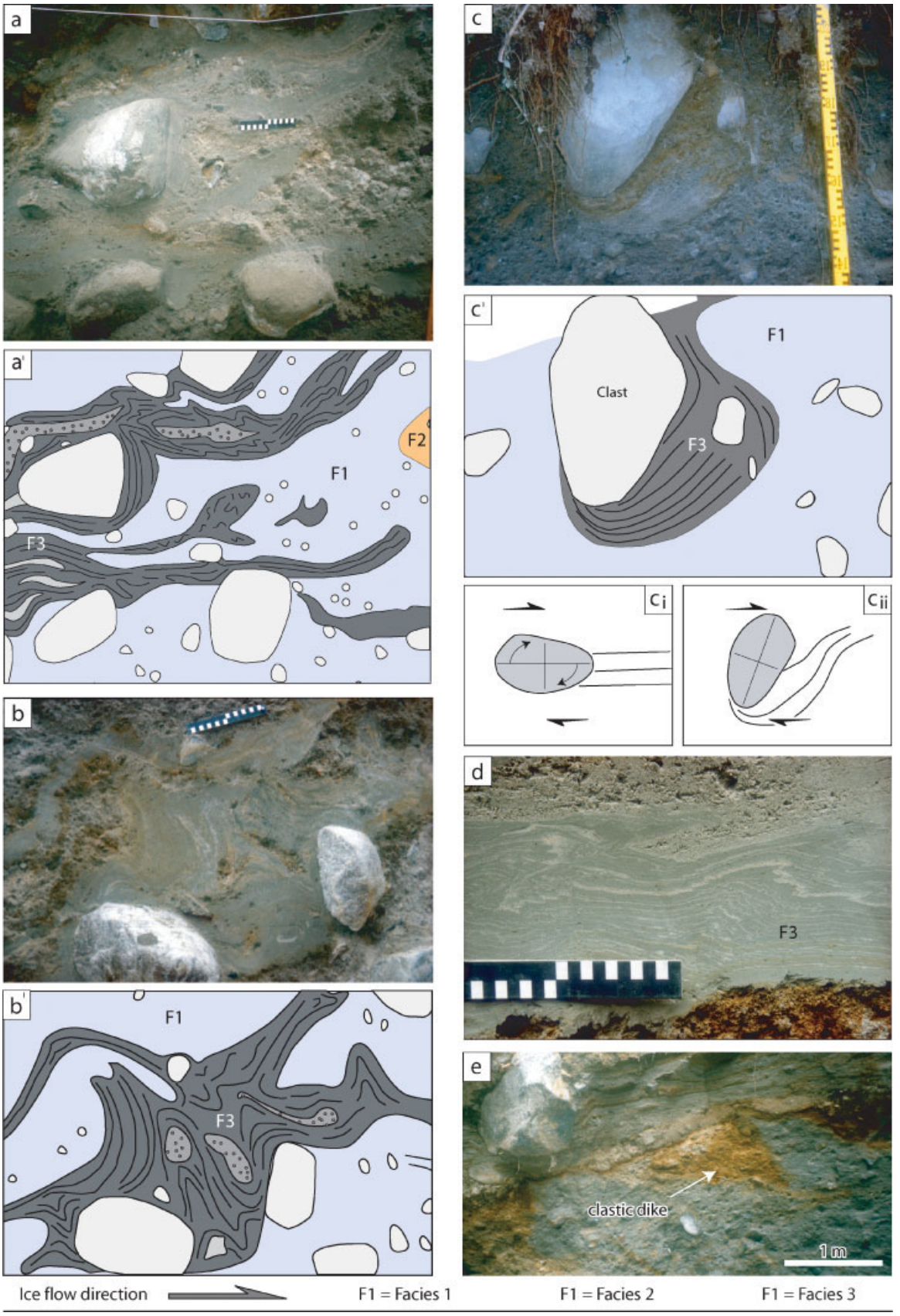

Figure 7 Sediment pictures and drawings containing mainly facies 1 and 3, and deformation structures. a/a′–b/b′. Deformed laminated sand and silt interbedded in sandy-silty deformation till. Primary sedimentary structures are preserved although deformed by shearing, folding, rotation, and ploughing. c/c′. Detailed picture and drawing of a rotated clast. The rotation by shearing is illustrated in c_i–c_{ii}. d. Small-scale folding and faulting of primary sedimentary structures in the laminated sand and silt (facies 3). e. A conjugate shear fracture forming a clastic dyke into facies 1 diamicton, filled with gravel and sand (emanates from onlapping facies 4 sediments; photo from trench wall opposite to the Ljusås 1 section, Fig. 4a). Facies 5 fine-grained sediments with a large dropstone (boulder) are seen to onlap in top of the picture

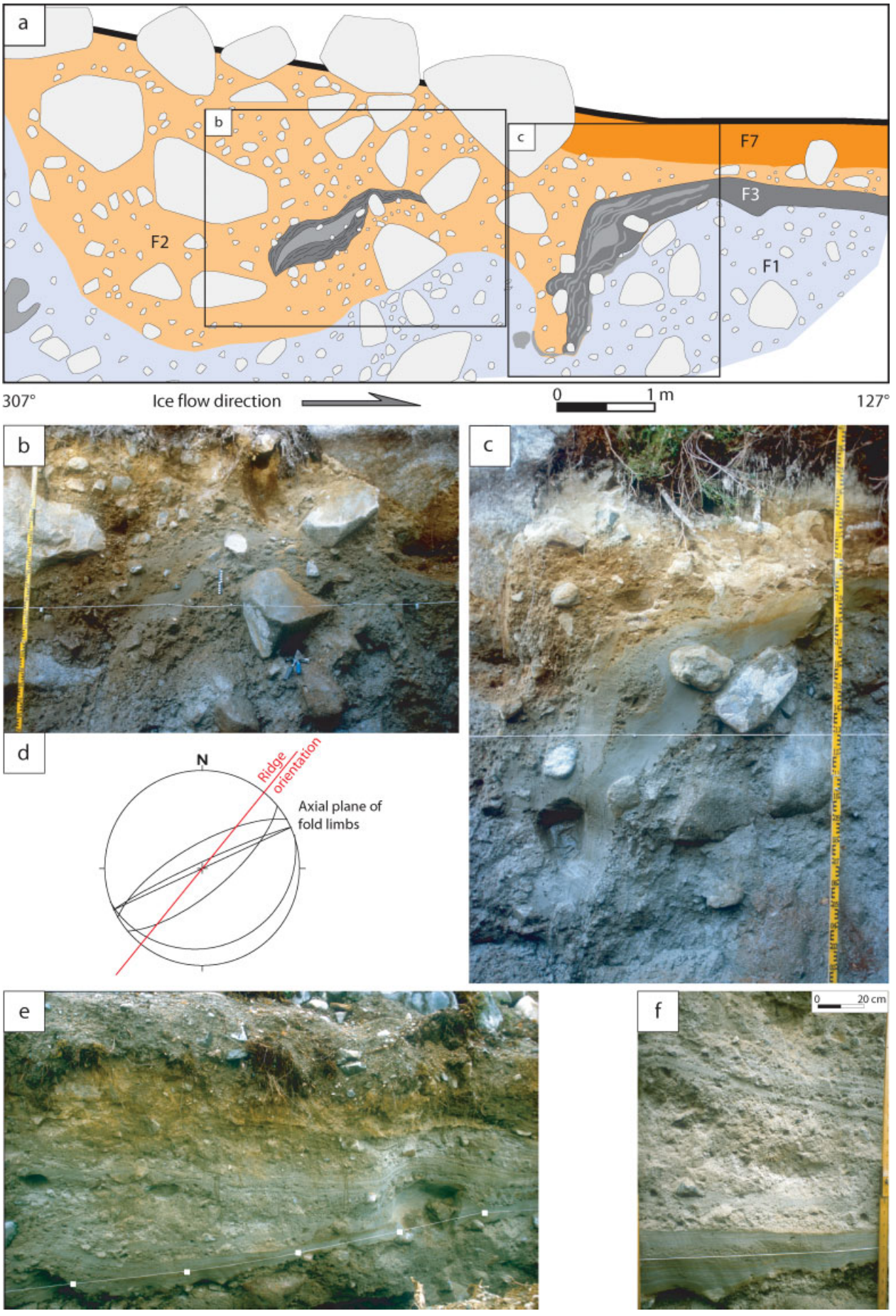

Figure 8 a. Detailed drawing of a synclinal fold in the distal part of section Rasmyran 2 (for legend, see Fig. 4). b–c. Pictures of details (marked in Fig. 8a). d. Plot of axial planes of folded beds within the section shown in Fig. 8a. e. Oblique photo of the distal part of section Ljuså 1 (Fig. 4a) with debris flow and glaciolacustrine deposits of facies 2 and 5, respectively, deposited on top of facies 3 (basically following the white string). The distance between white boxes on the string is 1 m. f. Close-up on facies 2 and 5 at mark 33 m in the Ljuså 1 section (Fig. 4a)

during large-scale folding of facies 1 and interbedded facies 3 sediments. This is evident at the Rasmyran 2 section; the four fabric analyses in this section (Fig. 5) are taken vertically above each other at approximately mark 25 m where facies 1 diamicton and overlying sediment form a compressional, open-fold structure (Fig. 4d, between marks 25–35 m, and Fig. 8). The lowermost fabric analyses (Rasmyran 2:1 and 2:2) show a very strong elongate fabric shape whereas the two upper analyses (Rasmyran 2:3 and 2:4), which are located in an anticlinal position within the diamicton, have lost most of their fabric strength.

The primarily waterlain facies 3 sediments are intimately related to facies 1 diamicton, one of the criteria making us interpret them as subglacial canal-infill sediments. The three-dimensional canal configuration is not easy to reconstruct from two-dimensional section walls. However, at places thicker and more extensive sorted sediment beds were exposed in both section walls of the trenches, 2–4 m apart. The sediments were thicker in one of the walls than in the other, indicating concave lower contacts transverse to flow direction. Some facies 3 beds are short along the projections of the section walls, being thicker in the middle and thinner towards both ends. All this suggests systems of broad (one metre to a couple of metres scale) but shallow (decimetre scale) canals, cut down into the underlying diamicton (facies 1), resembling the subglacial braided canal networks described by Walder and Fowler (1994) and Clark and Walder (1994). The existence of this subglacial fluvial distributary system shows that the basal melt-rate of the ice sheet, and thus the production of meltwater, was higher than could be drained by means of bulk movement of water within the deforming sediments (Clarke, 1987) and by darcian flow of the water through the pore spaces of the subglacial diamicton (Boulton and Jones, 1979; Boulton *et al.*, 1994), which due to its fine-grained composition has a low hydraulic conductivity. As indicated from the inter/intrabedding of facies 3 sorted sediments and facies 1 diamicton throughout the whole vertical sequence of a De Geer moraine, the canal drainage system followed the due to sediment accretion rising ice/bed interface, although migrating in time and space.

The sediment source for facies 3 might be threefold: erosion by meltwater at the ice–till interface, creep of diamict sediments from the contemporaneously deforming-bed system from outside into the canals when these were formed (cf. Walder and Fowler, 1994), and/or melt-out of debris from the canal roof. The coarser beds of facies 3 (gravelly sand and gravel) could represent residual deposits from all three types of sediment input. However, the predominating facies states are interbedded silt and fine sand, most likely deposited from suspension load at low to moderate, but fluctuating, stream velocities. Higher-velocity stream pulses are indicated by waning flow, normally graded sand beds, but traction-load bedforms were nowhere observed. The out-sized gravel and larger clasts, embedded within the fine-grained sediments, must be derived from the canal roof and deposited as dropstones (Thomas and Connell, 1985). The larger ones often show deformational load structures at their lower contacts but undisturbed onlap bedding of above-lying sediments.

The post-depositional deformation structures of different scales are characteristic for facies 3 sediments. When undeformed the contact to above-lying diamicton is sharp, indicating the development of a décollement surface at canal closure, while the small-scale deformation structures usually are connected to a gradational or folded upper contact to the diamicton (Fig. 7d), implying a stress transfer down into the facies 3 sediments beneath the reappeared deforming bed zone. However, as indicated from predominantly preserved primary bedding the cumulative strain induced into the facies 3 sediments were never large enough to cause a penetrative ductile deformation and can in this state be classified as a glacitectonite with just mildly distorted primary structures (Benn and Evans, 1996, 1998). Post-depositional deformation is also commonly occurring in connection with boulders. One type is associated with rotation of boulders, primarily deposited within facies 3 sediments but larger than bed thickness, thus protruding above the upper sediment contact after canal closure and therefore exposed to deforming bed conditions (Fig. 7c). The other type of deformation is connected to boulders in the deforming bed that were ploughed during deposition into facies 3 sediments.

Facies 2 diamicton is interpreted as reworked facies 1 deformation till, a rework leading to loss of the fine-grained constituents (ca. 75% of sediment <0.063 mm) and a transformation into a predominantly gravelly-sandy diamicton with increased clast concentrations. The interfingering contacts to facies 1 diamicton along the ridge crest-line suggest deposition at the marginal zone of a deforming bed during processes promoting winnowing out of fines from the parent diamicton. One process acting in this way would be reworking and subsequent removal of fines by subglacial meltwater that, in the frontal position, changed from a channelised system into a sheet-like drainage, possibly due to a slight buoyancy lift of the ice at and distal to the moraine ridge crest-line. At places this sorting process is interpreted to have been intense enough to change the parent material to clast-supported gravels, lying as diffuse bodies within the sandy-gravelly diamicton. In places where reworking was not complete, the preservation of sandy-silty lenses of diamicton enclosed within proximally situated gravelly-sandy diamicton was enabled.

The distal slope of ridge deposits is likely to have been unstable, directly owing to sediment failure and/or indirectly owing to ice push; the response in either case would be initiation of non-cohesive hyperconcentrated to concentrated density flows (Mulder and Alexander, 2001), as indicated by the distally inclined and out-pinching facies 2 beds, interbedded with facies 5 laminated sand and silt (for example, as in sections Ljusås 1 (Fig. 8e, f) and Rasmyran 1, of glaciolacustrine origin. The delivery of deforming bed diamicton (facies 1) at the ice margin would also result in gravity-driven density flows into the proglacial environment (cf. Lønne, 1995) once the ridge has started to build up. Erosive lower contacts of facies 2 beds into underlying facies 5 further support the density flow interpretation (Fig. 8f). The erosive nature of subaqueous density flows due to imposed shear stresses at their basal interface have been described both from modern environments and from ancient sediments (e.g. Eyles *et al.*, 1987; Prior and Bornhold, 1989; Lønne, 1993, 1995). Sorting processes with winnowing-out of fines should also be active during these flow stages; grain-to-grain interaction in the lower part and possibly turbid flow in the upper part of flow packages (Middleton, 1972; Postma *et al.*, 1988) will expel fine sands and silts into suspension (Lowe, 1982; Nemec *et al.*, 1984), later deposited as, for example, normally graded sand beds, here represented as facies 5. The massive structure of the facies 2 beds, the disorganised distribution of floating large clasts, and the absence of normal or inverse grading indicate a very low 'maturity' of these density flows, probably reflecting the short transport distance across the distal slope of the moraine ridge.

The deformation and folding of facies 2 sediments and interbedded facies 1 and 3 is most prominent in the central part, i.e. near the ridge crest-lines. Some of the deformation could be the result of loading due to rapid sediment deposition, although it is more likely that ice-induced stress is the main process as there is an increase of deformation towards the ice-proximal parts. Furthermore, the proximally predominant sandy-silty diamicton of facies 1, with silt and clay content up to 30%, is more likely to deform than distally laid facies 2.

On the proximal slope of the Ljusås 1 ridge, the onlapping facies 4 coarse-grained sediments imply traction bed-load and deposition at high flow velocities. Bed configurations in both section walls suggest a channelised flow with down-cutting into facies 1 diamicton. The wedge-shaped injections (Fig. 7e), emanating from this bed and forming clastic dykes, are found in the section wall with thin facies 4 sediments and are therefore situated closer to the lateral margin of the channel. This indicates that the fractures originate from glacial shearing and loading outside the channel, and that the fractures propagated into the substrate of the channel. The fractures are interpreted as conjugate shear fractures, suggested to represent brittle failure as a result of both the shear stress and the load applied by the ice, the shear stress component further enhanced by the up-glacier dip of the proximal ridge slope (Klint, 2001). Furthermore, the upward widening of the wedge structures is probably a response to upward-increasing induced shear stress (Fig. 7e). Owing to the lateral contact with the facies 4 sediment channel, sorted sediments were gradually filling the widening fractures, being syndepositional with the channel infill.

Facies 5: fine sand, silt and clay, interfingering with or onlapping ridge-forming sediments

Facies description. The sediments grouped into facies 5 were observed both in the proximal and distal parts of the Ljusås 1 section (Fig. 4). In Rasmyran 1 they were present just in the distal part of the section, whereas they were absent in all other sections. The lateral relationships to the ridge-forming facies 1–4 sediments are totally different with respect to location; facies 5 sediments onlap, and wedge out on the proximal side of the moraines, whereas they pinch out towards and interfinger with ridge-forming facies 2 sediments on the distal side (Figs. 8e and 8f). Unfortunately none of the trenches were long enough in proximal and distal directions to document these relations to be occurring everywhere.

On the proximal side of the Ljusås 1 ridge the facies 5 sediments form a fining upward sequence (maximum recorded thickness in section 50 cm), starting with laminated silt and fine sand with a sharp basal contact to underlying facies 4 sediments (Fig. 7e). They continue upwards into interlaminated silt and clay and eventually into massive silty clay, draped by facies 7 sands. Out-sized clasts occur, usually in gravel grades, but also some cobbles, 10–15 cm in diameter. In the opposite section wall at Ljusås 1 a boulder, ca. 1 m in diameter, was embedded in the sediments (Fig. 7e). The larger clasts are usually associated with deformation structures in the enclosing sediments as basal contact bending and small-scale folding.

In the distal parts of the sections Ljusås 1 and Rasmyran 1, facies 5 appears as thin beds (1–5 cm) or bedsets (up to 40 cm) of laminated to massive, sometimes normally graded, medium sand to silt. These beds are interbedded with facies 2 diamicton beds and, as the latter pinch out in the distal direction, the former grow gradually thicker with decreasing dip angles. The lower contacts to interbedded facies 2 are draping, whereas the upper contacts at places are slightly erosive. Small-scale deformation of primary sedimentary structures, and also of whole beds, are seen in conjunction with out-sized clasts, but also at a few places as overturned folds beneath overlying facies 2 diamicton.

Facies interpretation. Facies 5 represents deposition in the glaciolacustrine environment that gradually inundated the area during ice-margin retreat. Water depth at deglaciation of the excavated sites was 100–180 m. The interlaminated fine sand, silt and clay beds suggest that the primary process of deposition was suspension settling. As indicated from the interbedding with and close association to ridge-forming facies 2 diamicton, it is suggested that deposition was from low-density turbidity currents (cf. Lowe, 1982; Mulder and Alexander, 2001) that emanated close to the ice margin. Sediment sources for these density underflows were probably both the debouching subglacial drainage canals (containing facies 3) and the facies 2 concentrated to hyperconcentrated density flows at the moraine-ridge fronts, giving rise to secondary density flows during expelling and winnowing of fines (see above).

The distal-front exposures at Ljusås 1 and Rasmyran 1 show the 'active' interrelation between ridgeforming and non-ridge-forming sediment facies, whereas the facies 5 sediment succession at the proximal side of the Ljusås 1 ridge gives an example of the 'passive' relation. Here the sharp and onlapping contact to underlying facies 2 diamicton testifies to an abrupt change in depositional environment and the upward-fining sequence indicates increasing distance to the retreating ice margin. It is suggested that this abrupt shift in sedimentation is the result of a quick break-up of a grounding-line margin due to iceberg calving. Out-sized clasts within facies 5 sediment indicate sediment delivery also by ice rafting, though some of the embedded clasts in the ridge-frontal sediments could possibly be outrunners from gravity-induced processes.

Facies 6, surficial coarse-grained diamicton

Facies description. Facies 6 is predominantly a coarse-grained diamicton, appearing in the uppermost part of all sections, but most prominently seen in sections Ljusås 2:1 and Rasmyran 2 (Fig. 4). The bulldozing and destroying effect of the excavator disturbed and removed some of the facies 6 sediments, which explains their absence in some of the drawn sections. In general, facies 6 constitutes the ground surface of the moraine ridges and extends down to depths of 20–60 cm, with a diffuse contact to underlying facies 1 or 2 diamictons. The texture varies between sandy-gravelly diamicton to poorly sorted sandy gravel, always with a high content of large clasts. The concentration of boulders, embedded in or lying on top of the diamicton, changes laterally along the sections and is substantially higher at crests and on distal slopes.

Facies interpretation. Facies 6 is interpreted as a product of wave-reworking of the diamict sediments of facies 1 and 2. During a late stage of the glacial isostasy-driven regression, i.e. when moraine ridges were in a position between the wave base and the contemporary shoreline, they were exposed to significant reworking and redistribution of surface sediments and extraction of fines. Because of their position within the more large-scale topography, some ridge areas were more exposed to wave action than others. As shoreline regression was east-directed due to general slope of the terrain, the distal slopes of De Geer moraines were the ones that usually were exposed to the largest waves and storm fetch. This is indicated by a general trend for these slopes, together with ridge crestlines, to have higher boulder concentrations. The fine grains winnowed out by the waves were probably driven into suspension and brought further offshore, finally deposited as post-glacial silt and clay in low-energy environments, whereas sand and gravel fractions were deposited as facies 7 beach deposits in favourable positions (see below).

Facies 7, surficial sand and gravel

Facies description. Facies 7 constitutes massive and planar parallel-laminated beds of medium sand to fine gravel. It occurs in all trenches, but is restricted to the lowermost, flattened-out slopes on both the proximal and distal sides of the moraine ridges and is therefore usually outside the documented parts of the sections. When lower contacts to facies 2 or 5 sediments could be observed, they were found to be sharp but not erosive (no lag deposits). The facies 7 successions are usually thicker (up to 1 m) and more well-developed on the proximal sides of the ridges, and could often be traced into the basinal troughs between adjacent moraine ridges. This is especially prominent along and between the Rasmyran ridges, lying in a more elevated and exposed position than the Ljusså ridges.

Facies interpretation. Facies 7 is interpreted as beach deposits, composed of sediments removed from areas exposed to wave action. The source for facies 7 is thus all sediment surfaces containing these grain sizes, predominantly the moraine ridges themselves, but also adjacent till-covered hillsides and draping glaciolacustrine deposits. This means that deposition of facies 7 is synchronous with wave erosion at formation of facies 6.

The more frequent appearance and thicker accumulation of beach deposits on the proximal side of De Geer moraine ridges is probably due to a sheltering, lee-side effect provided by the moraine ridge, the inverted circumstances related to formation of facies 6. The more exposed distal side favoured erosion by wave action and partly prevented deposition of thicker facies 7 sequences; beach sediments were instead deposited on the lee side of the ridge. This phenomenon is evident from geological maps showing preferential deposition of beach deposits on NW-, SW- and NE-oriented slopes, slopes that were least affected by the general wave fetch from the southeast.

A depositional model for De Geer moraine formation

The model

Ridge-forming facies and their architectural relationships, and also their relations to ridge-distal facies, all indicate that De Geer moraines in the Boden area were formed along grounding lines associated with glacier retreat in a subaqueous environment. Thus they form ramp-like moraine ridges that are members of the morainal bank concept as proposed by, for example, Powell and Domack (1995). Furthermore, the De Geer moraine formation is associated with deforming bed transport of sediments to, and deposition at, the grounding line. Figure 9 proposes a four-stage sequential depositional model, in which different environments and processes are closely related to each other in time and space. Processes and products, and their relation to the grounding line, are listed in more detail in Table 2, presenting all processes thought to operate during ridge build-up, both erosional and depositional, and their associated products in a proximal–distal approach.

Stage 1. A subglacial deforming bed system, coupled to a superimposed migrating braided canal network (Fig. 9A) exists for some distance behind the retreating grounding line. Deformation till with highly developed clast orientation is deposited as a subglacial floor for the subsequently deposited De Geer moraines.

Stage 2. Up-glacier relocation of the grounding line is primarily due to ice-marginal calving. The subglacial system then becomes submarginal in relation to the grounding line and the deforming bed transport system changes to a predominantly depositional system (Fig. 9B) with constructional glaciotectonic deformation (Hart and Boulton, 1991), generating a local thickening of the subglacial bed, i.e. the initiation of De Geer moraine formation. The change into a predominantly depositional system is suggested to be a result of diminishing stress transfer from the ice into the substrate in the grounding-line direction; the deforming bed loses competence, 'freezing' the transport system and depositing the sandy-silty deformation till simultaneously with the glaciofluvial canal infill. The area immediately outside the grounding line is a glaciolacustrine environment, dominated by sediment gravity flows down the evolving distal slope of the moraine, suspension settling from underflows and deposition of melt-out debris from the ice-cliff and from icebergs (IRD). The sediments deposited in the pro-ridge glaciolacustrine system derive from direct deliverance by the deforming bed conveyor-belt and from debouching braided canal networks, and indirectly by redeposition due to sediment failure.

Stage 3. With a temporary stable grounding line, sediments are brought continuously from the subglacial environment to the submarginal–marginal zone where sediments are successively stacked, either as deformation till units on the proximal slope or as suspension settling and sediment gravity flow units on the distal slope (Fig. 9C). This results in a continuous vertical, but also proximal and distal build-up of a ramp-like moraine with a pronounced interfingering architecture of the discerned sedimentary units (facies 1–3) in the distal direction. Syn- and post-depositional deformation, seen as folding of beds or bedsets and plough deformation in association with large boulders, is abundant, predominantly in the proximal direction from ridge axes, representing varying stress-transfer penetration depths into sub-sole sediments.

Stage 4. After a new calving event and further up-glacier relocation of the grounding line, the former submarginal–marginal environment changes into an entirely glaciolacustrine one, dominated by suspension settling of fine-grained sediment from density underflows originating from the nearby new grounding line, incorporating varying amounts of ice-rafted debris. Contrary to the interfingering architecture of glaciolacustrine and moraine ridge sediments within the distal slope of the moraine, glaciolacustrine sediments now form an onlapping fining-upward succession of laminated sand and silt to massive silty clay in the proximal direction from ridge crest-line when depositional space is created due to calving-induced 'ice lift-off'. The fining-upward succession within the glaciolacustrine sediments indicates gradually increasing distance to the ice margin due to further grounding-line retreat.

Model comparisons

De Geer moraine sections in Norway, described by Larsen *et al.* (1991) and Blake (2000) reveal the same pattern of stacked sequences of diamicton and sorted sediment, all associated with syn- and post-depositional deformation and formation of moraines at grounding-line positions as described here from the Boden area. However, Larsen *et al.* (1991) stress ice-marginal push as the main process responsible for ridge formation and argues that the distribution pattern of the ridges supports a more or less annual formation at winter advances of the ice

Table 2 Grounding-line processes in De Geer moraine formation (partly based on Hunter *et al.*, 1996)

Process	Description	Contribution to sediment bodies and properties within and adjacent to grounding-line ridge
Subglacial		
Deforming bed	Down-glacier transfer of soft sediments below the glacier sole.	Repetitive deposition/stacking of deforming bed diamict units (facies 1) on proximal side of moraine.
Glaciofluvial transport/deposition	Braided canal networks beneath glacier sole with reworking and transport of sediments.	Canal infill of residual sediments and deposition of sediments from bedload and suspension transport (facies 3) in proximal and mid-ridge position.
Subglacial melt-out	Sediment release at the glacier sole.	Adds sediment to the transport/depositional system of facies 1 and 3; single larger clasts as 'dropstones' in facies 3.
Syn/post-depositional deformation	Stress transfer into sediments below glacier sole.	Non-penetrative deformation of facies 3 sediments, folding and thrusting of beds and bedsets of facies 1 and 3, boulder rotation and ploughing.
Ice marginal		
Mass movement	Sediment gravity flows at and distal to the grounding line, originating from direct delivery of deforming bed diamicton or indirectly due to sediment failure.	Repetitive vertical stacking of distally inclined diamict beds (facies 2) on distal side of the moraine. During flow stage a more or less pronounced winnowing-out of fines, forming a more coarse-grained diamict.
Ice-cliff melt-out	Surface melting in the ice cliff.	Release of debris, of which the coarser constituents are deposited along and distal to ridge axis and incorporated into facies 2 diamictons and ice-marginal units of facies 3 and 5 sorted sediments.
Calve dumping	Dumping of supraglacial debris during calving events.	Same as above.
Glaciofluvial bedload deposition	Canal mouths of the subglacial drainage network at grounding line.	Coarse-grained sediments debouch and spread out at the grounding line; build facies 3 beds interbedded with facies 2 diamicton.
Glaciofluvial erosion	Canal mouths of the subglacial drainage network at grounding line.	Erosion and winnowing of fines from facies 2 diamicton beds along ridge front.
Pro-marginal		
Density-flow settling	Suspended fine sediments in low-density turbidity currents in front of the grounding line.	Suspension settling, forming the glaciolacustrine facies association 5 sediments. Interbeds with facies 2 diamictons in distal part of the moraine ridge.
Iceberg rafting	Transport of debris in the distal direction from grounding line.	Do not contribute to ridge build-up; give out-sized clasts in distal facies 5 glaciolacustrine sediments.
Ice 'lift-off'	Ice-berg calving events.	Do not contribute to ridge build-up; creates depositional space in proximal direction from the former grounding, thus initiating deposition of onlapping facies 5 glaciolacustrine sediments.

margin. Formation of De Geer moraines at winter grounding-line advance is also proposed by Sollid and Carlsson (1984), based on ridge sedimentology much resembling that from the Boden area. However, these ridges lack evidence of glaciotectonic disturbances. Contrary to Larsen *et al.* (1991), Blake (2000) dismisses De Geer moraines as a chronological tool; each diamict bed with associated deformational structures in the stacked sequence of ridge sediments are taken as evidence for advance–retreat cycles of the grounding line over each particular De Geer moraine, the moraines therefore being potentially multi-annual. However, an alternative is suggested; the stacked sequence could also represent deposition during alternating settling and lifting off of the ice-front during one summer (Blake, 2000). The sedimentological data from the abovementioned investigations are all congruent with those from De Geer moraines in the Boden area and fit well within the proposed model, even though this model suggests deposition at temporary halts in the grounding-line retreat during the melt season. This will be further elucidated below in connection with discussions on grounding-line dynamics.

A large number of papers propose formation of De Geer moraines due to squeeze of water-saturated till into submarginal transverse crevasses (e.g. Elson, 1957; Hoppe, 1957, 1959; Andrews, 1963a, 1963b; Strömberg, 1965; Andrews and Smithson, 1966; Zilliacus, 1985, 1987, 1989; Lundqvist, 1989, 2000). However, none of these studies presents any sedimentological evidence for the proposed process. The only investigations on De Geer moraines that suggest deposition within submarginal crevasses and that are based on thorough sedimentological analysis are those of Beaudry and Prichonnet (1991, 1995). However, their model is not one of squeeze of till into crevasses. They suggest transport of diamict and sorted sediment to the proximal entrance of transverse crevasses, followed by deposition of down-glacier-inclined strata that show glaciotectonic structures as thrust faults and overturned to recumbent folds with up-glacier inclined planes. Firm diamicts are also preferentially deposited on the proximal side of the ridges. The described facies variability and sediment architecture from Beaudry and Prichonnet (1991, 1995) correspond well to those described for De Geer moraines in the Boden area and suggest that a grounding-line interpretation is equally adequate, especially as the sediments described do not reveal any evidence of confinement in the distal direction.

Independently of weak sedimentological evidence for subglacial crevasse infill in various ways, the weakest point in the crevasse concept seems to be the existence of the subglacial

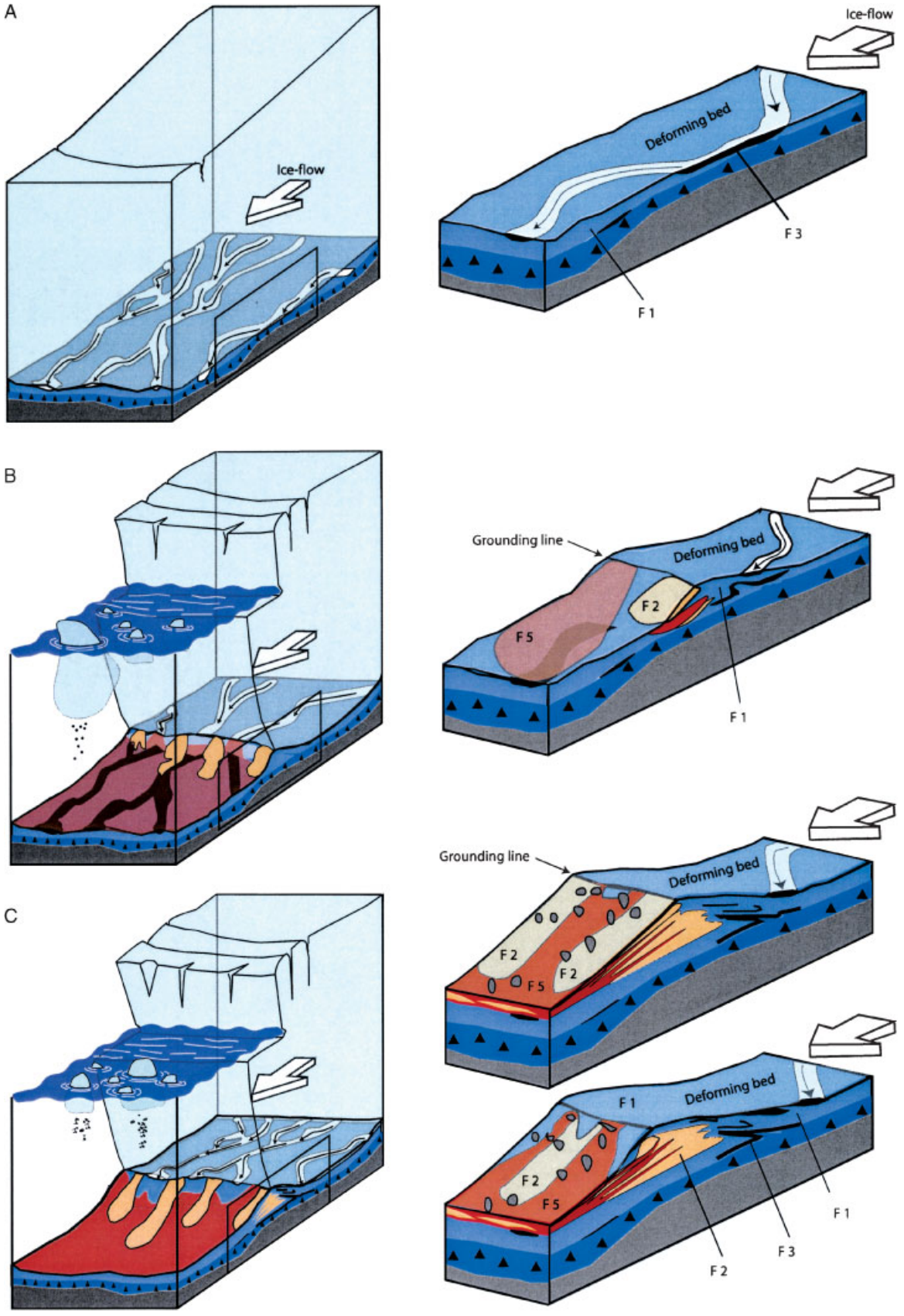

Figure 9 Depositional model of De Geer moraine formation. Stages A–C in the figure are related to stages 1–3 in the depositional-model text, respectively (for legend, see Fig. 4), whereas stage 4 in the text correspond to the onlapping glaciolacustrine sedimentation occurring distally of stages A–C in the figure

crevasses themselves. Blake (2000) gives a good review of their non-probability of existence and thus there is no need for repetition here. However, it must be noted that the crevasse patterns that Beaudry and Prichonnet (1991, 1995) take as analogues for their formation model, described from Antarctica by Jezek *et al.* (1979) and Jezek and Bentley (1983), are formed at, and distal to, the grounding-line of an ice shelf or at ice rises beneath the Ross Ice Shelf and are not proved to exist in the proximal direction from a grounding line.

Another possibility touched upon by De Geer (1940) for formation of subglacial crevasse systems is seismic activity in connection with isostatic rebound during the deglaciation. This

was further elucidated by Lundqvist (2000), arguing that the spatial distribution of De Geer moraines in Fennoscandia corresponds to known areas with high palaeoseismic activity. However, as it has not been proved by sedimentological evidence that De Geer moraines consist of crevasse-infill tills, as most existing sedimentological data point towards formation at retreating grounding lines and as seismicity-induced crevasse pattern cannot explain the topography-dependent spatial distribution and undulating configuration of De Geer moraine tracts, it must be ruled out that palaeoseismic activity has anything to do with De Geer moraine formation *sensu stricto*, other than possibly triggering major calving events.

Implications on ice sheet retreat and grounding line dynamics—a discussion

The large-scale picture

The final deglaciation of roughly one-quarter of the Scandinavian ice sheet took place with an average recession rate of 400 m yr^{-1}, calculated along a flow line from Salpausselkä in the south, across the Gulf of Bothnia and to coastal northern Sweden, a recession rate sustained for ca. 2000 years. The deglaciation along the abovementioned flow line took place at ice-marginal water depths of 200–300 m, first during a short period of marine-brackish conditions (e.g. Björck, 1995), the Yoldia phase of the Baltic basin, but mostly during freshwater lacustrine conditions, the Ancylus Lake phase. Continuous formation of De Geer moraines at the retreating ice margin seems not to have been the case as these turn up in a patchy distribution pattern over southwestern Finland (cf. Zilliacus, 1987). De Geer moraines would be expected on the bottom of the Gulf of Bothnia as an extension of the abundant occurrences in the Vasa district, Finland. This seems, however, not to be the case according to seismic studies by Andrén (1990). De Geer moraines in abundance turn up again on emerged—and emerging—coastal areas of northern Sweden along the Gulf of Bothnia. The distribution pattern of De Geer moraines therefore indicates that favourable conditions for moraine ridge formation were not always present during ice-margin retreat.

The abovementioned retreat rate as such is not exceptional, as much higher ones have been reported from modern settings in water-terminating glaciers (e.g. Warren, 1992; van der Veen, 1996). However, most monitoring is on topography-bound outlet glaciers and the monitored time is short, so possibly there is no reliable, modern analogy to the fast and spatially extensive down-wasting of the southeastern flank of the Scandinavian Ice Sheet. Calving along a grounded ice cliff is regarded as the predominating ablation process of water-terminating glaciers. Estimates from Greenland (Reeh, 1994) and Antarctica (Jacobs *et al.*, 1992) suggest that calving accounts for about 56% and 77% of the total mass loss, respectively. Surface, ice cliff and basal melting thus seem to be of a second order of importance, though the large and frequently occurring beaded esker systems north of the Swedish/Finnish Younger Dryas ice-marginal zone testifies the importance of extensive surface melting and well-developed subglacial drainage systems during the final deglaciation. The calving rate is balanced by the ice flux towards the margin; if equal the margin would be in a stable position. As this is not the case, as shown by the recession data, the calving rate must have been greater than the ice flux towards the margin, the latter determined by the iceflow velocity.

The calving processes at water-terminating glaciers—and forces driving the process(es)—are not fully understood and seem to be quite complex (e.g. Warren, 1992; van der Veen, 1996). Based preferentially on studies of tidewater glaciers, it is commonly accepted that there is a strong linear relation between calving rate and water depth at grounded ice margins (Brown *et al.*, 1982), but that the absolute values of calving rate in this relation is an order of magnitude smaller in a lacustrine environment, compared to a marine environment (Funk and Röthlisberger, 1989). The higher calving rate for tidewater glaciers has been attributed to a number of physical differences, for example higher buoyancy in saltwater, a larger exposure to waves and storms, high tidal flexure and enhanced ice-cliff melting in saltwater (Warren, 1992). If the linear relation between calving rate and water depth holds true this would mean that a glacier with constant ice flux along its margin would calve back faster where it is situated in deep water, compared to areas where the grounded ice cliff is standing in shallower water. This process might be demonstrated by the fact that De Geer moraine distribution often suggests an undulating concave/convex ice-margin configuration, most clearly developed as deep embayments around nearly all subaqueous eskers north of the Swedish Younger Dryas ice-marginal zone, interpreted as calving bays with enhanced calving in the deepest part of the bottom topography, which also is the location for the eskers (Strömberg, 1981, 1989).

This undulating ice-marginal configuration can also be seen in Norrbotten, mirrored in the distribution pattern of De Geer moraines. In the flat coastal areas the De Geer moraines indicate a quite linear ice margin, whereas further towards the northwest with increasing relative relief of the landscape—and thus different water depths in front of the receding ice margin—the configuration of De Geer moraines suggests more or less evident embayment within the major valleys and protruding ice margins over high ground. Measurements over a number of adjacent valleys in the Boden area show maximum indentations, calculated from a hypothetical linear ice margin, of 200–800 m over 2–6 km ice-marginal length. These valleys experienced maximum water depths of around 150–200 m at deglaciation. Taking the calving rate/water depth equation (Funk and Röthlisberger, 1989; Warren, 1992) for freshwater at face value and excluding compensation for calving mass-loss by means of ice flux towards the margin, water twice as deep in valleys than over the interfluves would create an undulation of the ice margin much larger than that indicated above from the De Geer moraines. This undulation would also increase exponentially in time due to a cumulative effect which suggests that the calving process—and rate—is strongly counterbalanced by iceflow towards the ice margin, and that the ice flux is higher in the valleys than over higher ground.

The assumption that the annual mean calving rate has just a simple linear relation to increase in water depth at the terminus has been challenged by van der Veen (1996), arguing that this calving law is based on circumstantial evidence. Instead it was suggested that increasing calving rate and glacier retreat is linked to increasing glacier speed and the associated thinning of the glacier. Data from Columbia Glacier, Alaska (van der Veen, 1996), indicate that the terminus retreats if the ice thickness in excess of flotation becomes less than a critical value, which here seems to be in the order of 50 m above flotation thickness for steady-state conditions. Thus calving rate becomes a secondary parameter, determined by thinning rate at the glacier margin due to iceflow velocity and not primarily by the water depth, and the focus is then changed to processes along the glacier bed.

Our sedimentological data and model of De Geer moraine formation indicate advection of deforming bed sediments towards the grounded ice margin where a gradually thickening wedge of till is deposited owing to decreasing effective stress,

eventually being close to flotation pressures (i.e. zero effective stress at the base of the glacier). The sedimentological evidence of an existing deforming bed also suggests fast iceflow, promoting thinning of the ice and therefore enhancing calving processes according to the ideas suggested by van der Veen (1996). The existence of a wide infra-marginal zone with deforming bed conditions is also supported by Kleman *et al.* (1997) who, on the basis of aerial photographic interpretation of glacial landforms, identified a wet-based deglacial fan over the investigation area.

Our ongoing studies on Niemisel moraines (Lindén and Möller, in preparation) also support the deforming bed concept; occasionally De Geer and Niemisel moraines occur in the same areas, the former landforms always superimposed on the latter, which shows their relative age relation. Niemisel moraine ridges are built up in their proximal part by thrust and folded slabs of sorted sediments and by glacitectonites (deforming bed sediments; Benn and Evans, 1996), and the whole landform is draped with a late-stage bed of deformation till, indicating a broad area with deforming bed conditions. The occurrence of Niemisel moraines in the lowest parts of the valleys coincides with the distribution of the largest and most continuous De Geer moraines; the latter are also found on higher ground but become lower and more discontinuous if they continue up valley sides and over interfluves, and become almost absent at altitudes above 150 m a.s.l., which corresponds to water depths of ca. 70 metres at deglaciation (Fig. 3a). These relations can be interpreted in terms of sediment flux and thus also iceflow velocities. Valleys promote higher iceflow velocities and thus higher sediment fluxes, giving rise to higher and more continuous De Geer moraines at the grounded ice margin and infra-marginal draping of deforming bed till over previously deposited Niemisel moraines, at the same time promoting a high calving rate and ice-margin embayment due to glacier thinning. High ground would experience the opposite relations with a subglacial environment incompatible with Niemisel moraine formation and weak conditions for marginal De Geer moraine formation, which more or less totally stops at water depths less than ca. 70 m, suggested to be due to insufficient sediment flux.

Grounding-line dynamics

The original idea of De Geer (1889) was that annual subaquatic moraines were formed during a winter advance of the grounded ice margin, pushing up a ridge of available sediments in front of the glacier. If the next winter advance did not reach the previous winter position the distance between two adjacent ridges should mark the net retreat, i.e. summer retreat minus winter advance of that year. However, this quite logical hypothesis was not based on any field evidence, until more recent work by, for example, Powell (1981) and Boulton (1986). From Aavatsmarkbreen, Spitsbergen, Boulton (1986) demonstrated how a winter advance in subaerial position, here marked by a push-moraine formed from proglacial sand and gravel could be followed into its subaquatic continuation, here marked by buckled and overthrust sea ice along the ice cliff. Sonar profiles on the sea bed in front of the glacier revealed a series of well-defined, up to 10 m high, till ridges which accordingly were interpreted to be annually formed push-moraines of former winter advances. As the number of ridges fitted perfectly to the monitored time slice—seven years with a calculated mean retreat rate of 40 m yr^{-1}—there is a strong case for these ridges being annual. Winter advance of grounded ice margins have been reported from a number of modern settings (e.g. Powell, 1981; Boulton, 1986; van der Veen, 1996), which can be explained by an ice flux towards the margin during winter that is larger than the mass loss, preferentially by calving. Winter calving is suppressed by, for example, obstruction from frontal sea/lake ice, also reducing thermal and physical notch erosion at the water line (Kirkbride and Warren, 1997), freezing of water in terminal crevasses (Boulton, 1986) and winter decrease of iceflow which in turn reduce crevasse-forming tensional stress (Warren *et al.*, 1995).

Our sedimentological data and model of De Geer moraine formation do not support this annual winter-advance push-moraine formation. Instead, the De Geer moraines in the Boden area suggest active sediment deposition at temporary, quite short-lived, grounding-line positions during summer retreat, driven preferentially by calving processes. However, we think that both models can be neatly put together, indicating the complexity of De Geer moraine formation at the grounding line, instead of elaborating with basal crevasses to produce moraines with no relative geochronological value (Beaudry and Prichonnet, 1995). In areas with favourable conditions for advection of deforming bed sediments (and glaciofluvially transported sediments) to temporary grounding-line stillstands a varying number of 'summer moraines' are formed during general ice-margin retreat. During winter, with a highly suppressed calving rate, possibly reaching zero, the grounding line advances. Depending on the spacing between the previously deposited summer moraines, a number of them are erased and possibly a terminal push-moraine of that winter advance is formed, a 'winter moraine'. This erasure of previously deposited moraines has been demonstrated by Boulton (1986) from a modern fjord setting on Baffin Island, arctic Canada, where only 40 moraines from 60 to 100 years of retreat of the glacier have survived owing to the slow mean retreat rate and the quite large and varying winter advances.

A De Geer moraine formed primarily by marginal pushing should be recognisable from its internal structures. None of our studied sections reveal such structures, and we therefore suggest that our trenches by mere chance were laid out only over summer moraines, which by their number should be the predominating moraines in this area. However, winter moraines should be expected somewhere, integrated with summer moraines.

Calving dynamics

If grounding-line retreat was just due to a continuous calving, then there would be no time for wedge-like sediment build-up along clearly defined lines, but just an indifferent sediment delivery at the grounding-line, not recognised as ridges. Our model of De Geer moraine formation stresses the importance of grounding-line activity and indicates that there must have been a stepwise marginal retreat, steps being in the order of 150–200 m, as indicated by the mean distance between ridges, but sometimes as short as 50 m. On the other hand, in areas devoid of moraine ridges—which is common within predominating De Geer moraine tracts—the opposite would then be the case, i.e. just gradual ice-margin retreat with insufficient time for moraine ridge build-up within localised areas.

The calving mechanism of water-terminating glaciers has been described by, for example, Warren (1992), Warren *et al.* (1995), Kirkbride and Warren (1997) and Hughes (2002). In summary, the processes can be categorised into slab and flake calving above the waterline, and large-scale block calving below the waterline (Fig. 10). The former include full-height slab calving, emanating from cliff-parallel vertical surface

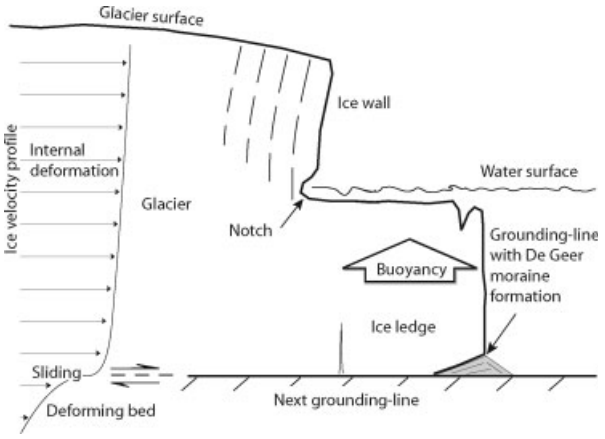

Figure 10 Cartoon showing calving mechanisms above and below the waterline and formation of a subaqueous ice ledge (modified from Hughes, 2002). Position of deposition of De Geer moraines at the margin in the figure is moved in proximal direction as the ice ledge calves back

cracks, but also calving of smaller blocks of ice above notches produced by thermal erosion along the waterline. Both types of calving above or close to the waterline interact into formation of a submarine ledge (Hughes, 2002) which calves upwards when buoyancy stresses are large enough to produce a fracture that can free the ice-block from the main ice cliff. According to Hughes (2002), ice ledges theoretically calve along produced bottom crevasses when the width of the ledge approaches half of the ice thickness below water. If correct, for common water depths at deglaciation in the Boden area this would produce icebergs 50–100 m wide measured perpendicularly to the ice cliff and thus also grounding-line recessional steps of the same magnitude. The mechanisms described for ice-cliff retreat match our proposed model for De Geer formation, even though the relationship between water depth and ice ledge width at break-off seems to be larger than proposed by Hughes (2002) if ice ledge calving just happens in one step. The absence of any tidewater effect at deglaciation of the Boden area and also the reduced buoyancy effect owing to freshwater and not saltwater in the Ancylus Lake can be parameters explaining a somewhat wider ice ledge before break-off in this kind of environment. The process of ice-ledge formation gives time for ridge build-up at a temporarily stable subaqueous grounding line, at the same time as the subaerial part of the ice cliff calves back, forming the submarine ledge. When the ledge eventually breaks off because of buoyancy forces, the grounding-line sediment accretion comes to an abrupt halt, depositional space is created for onlapping lacustrine sediments in the proximal direction from the previous grounding line and a new temporarily stable grounding line is established, starting the process again.

Conclusions

- De Geer moraines form during temporary halts in grounding-line retreat of water-terminating ice sheet margins, preferentially during the summer season, as a result of subglacial sediment advection to the ice margin.
- De Geer moraines most probably also form during winter readvances of the ice margin as push moraines, though this is not supported from our field studies.
- The proximal part of De Geer moraines is built up in a submarginal position as stacked sequences of deforming bed diamictons intercalated with glaciofluvial canal-infill sediments, all associated with both syn- and post-depositional deformation.
- The distal part of De Geer moraines is dominantly built up from the grounding line by prograding sediment gravity flow deposits, distally interfingering with fine-grained sediments deposited in the frontal glaciolacustrine environment.
- The rapid marginal recession rate (ca. 400 m yr^{-1}) is suggested to be driven by rapid calving, in turn enhanced by fast iceflow and marginal thinning of the ice due to deforming bed conditions.
- The stepwise retreat of grounding lines, as indicated by the spatial distribution of De Geer moraine ridges, suggests subaqueous ice-ledge calving to a new grounding-line position, followed by regained sediment delivery and ridge build-up.
- The spatial distribution of De Geer moraines in Norrbotten, northern Sweden, suggest an average formation/preservation of 2–3 'summer moraine' ridges every year, possibly intercalated with a push-ridge formed during winter advance.

Acknowledgements This work was supported by the Geological Survey of Sweden by a 3-year grant to Per Möller (contract no. 03-1145/2000). Kurt H. Kjær and Lena Adrielsson critically read the manuscript and gave valuable suggestions for improvements. Kevin Gustavson and an anonymous reviewer forced us to strengthen our arguments. The SCA (Svenska Cellulosa Aktiebolaget) gave us permission to exercise 'brutal geology' when excavating De Geer moraines on their property in the Ljusåa area and so did the Vestman family in Rasmyran. Our sincere thanks are forwarded to all of them.

References

Andrén T. 1990. Till stratigraphy and ice recession in the Bothnian Bay. University of Stockholm. *Department of Quaternary Research, Report* **18**; 59 pp.

Andrews JT. 1963a. Cross-valley moraines of the Rimrock and Isortoq valleys, Baffin Island, N.W.T: a descriptive analysis. *Geographical Bulletin* **5**: 49–77.

Andrews JT. 1963b. The cross-valley moraines on north-central Baffin Island: a quantitative analysis. *Geographical Bulletin* **20**: 82–129.

Andrews JT, Smithson BB. 1966. Till fabrics of the cross-valley moraines of north-central Baffin Island, Northwest Territories, Canada. *Geological Society of America Bulletin* **77**: 271–290.

Beaudry LM, Prichonnet G. 1991. Late Glacial De Geer moraines with glaciofluvial sediment in the Chapais area, Québec (Canada). *Boreas* **20**: 377–394.

Beaudry LM, Prichonnet G. 1995. Formation of De Geer moraines deposited subglacially, central Québec. *Géographie Physique et Quaternaire* **49**: 337–361.

Benn DI. 1994. Fabric shape and the interpretation of sedimentary fabric data. *Journal of Sedimentary Research* **A64**: 910–915.

Benn DI. 1995. Fabric signature of subglacial till deformation, Breidamerjökull, Iceland. *Sedimentology* **42**: 735–747.

Benn DI, Evans JA. 1996. The interpretation and classification of subglacially-deformed materials. *Quaternary Science Reviews* **15**: 23–52.

Benn DI, Evans JA. 1998. *Glaciers and Glaciation*. Arnold: London; 734.

Bergström R. 1968. Stratigrafi och isrecession i södra Västerbotten. Swedish Geological Survey C, *634*; 76 pp.

Beskow G. 1935. Praktiska och kvartärgeologiska resultat av grusinventeringen i Norrbotten. *Geologiska Föreningens i Stockholm Förhandlingar* **57**: 120–123.

Björck S. 1995. A review of the history of the Baltic Sea, 13.0–8.0 ka BP. *Quaternary International* **27**: 19–40.

Blake KP. 2000. Common origin for De Geer moraines of variable composition in Raudvassdalen, northern Norway. *Journal of Quaternary Science* **15**: 633–644.

Boulton GS. 1986. Push-moraines and glacier-contact fans in marine and terrestrial environments. *Sedimentology* **33**: 677–698.
Boulton GS. 1996. Theory of glacial erosion, transport and deposition as a consequence of subglacial sediment deformation. *Journal of Glaciology* **42**: 43–62.
Boulton GS, Hindmarsh RCA. 1987. Sediment deformation beneath glaciers: rheology and sedimentological consequences. *Journal of Geophysical Research* **92**: 9059–9082.
Boulton GS, Jones AS. 1979. Stability of temperate ice caps and ice sheets resting on beds of deformable sediments. *Journal of Glaciology* **24**: 29–43.
Boulton GS, Slot T, Blessing G, Glasbergen P, Leijnse T, van Gijssel K. 1994. Deep circulation of ground water in overpressured subglacial aquifers and its geological consequences. *Quaternary Science Reviews* **12**: 739–745.
Boulton GS, Dobbie KE, Zatsepin S. 2001a. Sediment deformation beneath glaciers and its coupling to the subglacial hydraulic system. *Quaternary International* **86**: 3–28.
Boulton GS, Dongelmans P, Punkari M, Broadgate M. 2001b. Palaeoglaciology of an ice sheet through a glacial cycle: the European ice sheet through the Weichselian. *Quaternary Science Reviews* **20**: 591–625.
Brown CS, Meier MF, Post A. 1982. Calving speed of Alaska tidewater glaciers, with application to Columbia Glacier. U.S.G.S. Professional Paper, 1258-C.
Clark PU, Walder JS. 1994. Subglacial drainage, eskers, and deforming beds beneath the Laurentide and Eurasian ice sheets. *Geological Society of America Bulletin* **106**: 304–314.
Clarke GKC. 1987. Subglacial till: a physical framework for its properties and processes. *Journal of Geophysical Research* **92**: 9023–9036.
De Geer G. 1889. Ändmoränerna i trakten mellan Spånga och Sundbyberg. *Geologiska Föreningens i Stockholm Förhandlingar* **11**(126): 395–396.
De Geer G. 1940. Geochronologia Suecica Principles. Kungliga Svenska Vetenskapsakademiens Handlingar III:18:6; 367 pp.
Dionne JC, Shilts WW. 1974. A Pleistocene clastic dike, upper Chaudiere valley, Quebec. *Canadian Journal of Earth Sciences* **11**: 1594–1605.
Donner J. 1995. *The Quaternary History of Scandinavia*. Cambridge University Press: Cambridge; 200.
Elson JA. 1957. Origin of wash-board moraines. *Geological Society of America Bulletin* **68**: 1721.
Eriksson L, Henkel H. 1994. Geophysics. In *Geolog: National Atlas of Sweden*, Fredén C (ed.). Almqvist & Wiksell International: Stockholm; 208.
Eyles N, Eyles CH, Miall AD. 1983. Lithofacies types and vertical profile models: an alternative approach to the description and environmental interpretation of glacial diamict and diamictite sequences. *Sedimentology* **30**: 393–410.
Eyles N, Clark BM, Clague JJ. 1987. Coarse-grained sediment-gravity flow facies in a large supraglacial lake. *Sedimentology* **34**: 193–216.
Fischer UH, Clarke GKC. 2001. Review of subglacial hydro-mechanical coupling: Trapridge Glacier, Yukon Territory, Canada. *Quaternary International* **86**: 29–43.
Fromm E. 1965. Beskrivning av jordartskarta över Norrbottens län nedan lappmarksgränsen. Swedish Geological Survey, Ca 39; 232 pp.
Funk M, Röthlisberger H. 1989. Gletcher-Kalbungsgeschwindigkeit im Süsswasser: eine Studie am Nordbogletcher im Johan Dahls Land, Süd-West Grönland. *MitteilungVAW/ETHZ* **20**: 1–47.
Gråsäs K. 1990. Jordartkarta 25L Boden NV. Swedish Geological Survey, Ak 17.
Hart JK. 1994. Till fabric associated with deformable beds. *Earth Surface Processes and Landforms* **19**: 15–32.
Hart JK, Boulton GS. 1991. The interrelation of glaciotectonic and glaciodepositional processes within the glacial environment. *Quaternary Science Reviews* **10**: 335–350.
Hart J, Rose J. 2001. Approaches to the study of glacier bed deformation. *Quaternary International* **86**: 45–58.
Hättestrand C. 1997. The glacial geomorphology of central and northern Sweden. Swedish Geological Survey, Ca 85; 47 pp.
Hoppe G. 1948. Isressessionen från Norrbottens kustland. *Geographica* **20**: 1–112.
Hoppe G. 1952. Hummocky moraine regions, with special reference to the interior of Norrbotten. *Geografiska Annaler* **33**: 157–165.
Hoppe G. 1957. Problems of glacial geomorphology and the Ice Age. *Geografiska Annaler* **39**: 1–18.
Hoppe G. 1959. Glacial morphology and inland ice recession in northern Sweden. *Geografiska Annaler* **41**: 193–212.
Hughes T. 2002. Calving bays. *Quaternary Science Reviews* **21**: 267–282.
Hunter LE, Powell RD, Lawson DE. 1996. Morainal-bank sediment budgets and their influence on the stability of tidewater termini of valley glaciers entering Glacier Bay, Alaska, USA. *Annals of Glaciology* **22**: 211–216.
Jacobs SS, Helmer HH, Doake CSM, Jenkins A, Frolich RM. 1992. Melting of ice shelfs and the mass balance of Antarctica. *Journal of Glaciology* **38**: 375–387.
Jezek CK, Bentley C. 1983. Field studies of bottom crevasses in the Ross Ice Shelf, Antarctica. *Journal of Glaciology* **29**: 118–126.
Jezek CK, Bentley C, Clough J. 1979. Electromagnetic sounding of bottom crevasses on the Ross Ice Shelf, Antarctica. *Journal of Glaciology* **24**: 321–330.
Kirkbride MP, Warren CR. 1997. Calving processes at a grounded ice cliff. *Annals of Glaciology* **24**: 116–121.
Kleman J. 1990. On the use of glacial striae for reconstruction of paleo-ice flow patterns—with application to the Scandinavian ice sheet. *Geografiska Annaler* **72A**: 217–236.
Kleman J. 1992. The palimpsest glacial landscape in northern Sweden—Late Weichselian deglaciation landforms and traces of older west-centred ice sheets. *Geografiska Annaler* **72A**: 305–325.
Kleman J, Hättestrand C, Borgström I, Stroeven A. 1997. Fennoscandian palaeoglaciology reconstructed using a glacial inversion model. *Journal of Glaciology* **43**: 283–299.
Klint KES. 2001. Fractures in glacigene diamict deposits: origin and distribution. Danmarks og Grönlands Geologiske Undersökelse, Report 2001/129; 360 pp.
Larsen E, Longva O, Follestad BA. 1991. Formation of De Geer moraines and implications for deglaciation dynamics. *Journal of Quaternary Science* **6**: 263–277.
Lawson DE. 1982. Mobilization, movement and deposition of active subaerial sediment flows, Matanuska Glacier, Alaska. *Journal of Geology* **90**: 279–300.
Lønne I. 1993. Physical signatures of ice advance in a Younger Dryas ice-contact delta, Troms, northern Norway: implications for glacier-terminus history. *Boreas* **22**: 59–70.
Lønne I. 1995. Sedimentary facies and depositional architecture of ice-contact glaciomarine systems. *Sedimentary Geology* **98**: 13–43.
Lowe DR. 1982. Sediment gravity flows: II. Depositional models with special reference to the deposits of high-density turbidity currents. *Journal of Sedimentary Petrology* **52**: 279–297.
Lundqvist J. 1981. Moraine morphology—terminal remarks and regional aspects. *Geografiska Annaler* **63A**: 127–137.
Lundqvist J. 1989. Late glacial ice lobes and glacial landforms in Scandinavia. In *Genetic Classification of Glacigenic Deposits*, Goldthwait RP, Matsch CL (eds). A. A. Balkema: Rotterdam; 217–225.
Lundqvist J. 1992. Glacial stratigraphy in Sweden. Geological Survey of Finland, Special Paper No. 15; 43–59.
Lundqvist J. 1994. The deglaciation. In *Geology, National Atlas of Sweden*, Fredén C (ed.). Almqvist & Wiksell: Stockholm; 208.
Lundqvist J. 2000. Palaeoseismicity and De Geer Moraines. *Quaternary International* **68–71**: 175–186.
Lundqvist J, Wohlfarth B. 2001. Timing and east–west correlation of south Swedish ice marginal lines during the Late Weichselian. *Quaternary Science Reviews* **20**: 1127–1148.
Mark DM. 1973. Analysis of axial orientation data, including till fabrics. *Geological Society of America Bulletin* **84**: 1369–1374.
Mawdsley JB. 1936. The wash-board moraines of the Opawica-Chibougamau Area Quebec. *Transactions of the Royal Society of Canada* **3**(30): 9–12.
Middleton MA. 1972. The role of subaqueous debris flows in generating turbidity currents. *Journal of Sedimentary Petrology* **42**: 775–793.
Möller H. 1962. Annuella och interannuella ändmoräner. *Geologiska Föreningens i Stockholm Förhandlingar* **84**: 134–143.

Mulder T, Alexander J. 2001. The physical character of subaqueous sedimentary density flows and their deposits. *Sedimentology* **48**: 269–299.

Nemec W, Steel RJ, Porebski SJ, Spinnangr X. 1984. Domba Conglomerate, Devonian, Norway: process and lateral variability in a mass flow-dominated, lacustrine fan-delta. In *Sedimentology of Gravels and Conglomerates*, Koster EH, Steel RJ (eds). Canadian Society of Petroleum Geologists, Memoir No. 10; 295–320.

Norman GWH. 1938. The last Pleistocene ice front in Chibougamau district, Quebec. *Transactions of the Royal Society of Canada* **3**(32): 69–86.

Postma G, Nemec W, Kleinspehn KL. 1988. Large floating clasts in turbidites: a mechanism for their emplacement. *Sedimentary Geology* **58**: 47–61.

Powell R. 1981. A model for sedimentation by tidewater glaciers. *Annals of Geology* **2**: 129–135.

Powell R, Domack E. 1995. Modern glaciomarine environments. In *Modern Glacial Environments—Processes, Dynamics and Sediments*, Vol. 1, Menzies J (ed.). Butterworth Heinemann: Oxford; 445–486.

Prest VK. 1968. Nomenclature of moraines and ice-flow features as applied to the map of Canada. Geological Survey of Canada, Papers 67–57; 32 pp.

Prior DB, Bornhold BD. 1989. Submarine sedimentation on a developing Holocene fan delta. *Sedimentology* **36**: 1053–1076.

Reeh N. 1994. On the calving of ice from floating glaciers and ice shelfs. *Journal of Glaciology* **7**: 215–232.

Rodhe L, Svedlund JO. 1990. Jordartkarta 25L Boden SV. Swedish Geological Survey, Ak 14.

Siegert MJ, Dowdeswell JA. 2002. Late Weichselian iceberg, surface melting and sediment production from the last Eurasian Ice Sheet: results from numerical ice-sheet modelling. *Marine Geology* **188**: 109–127.

Sollid JK, Carlsson AB. 1984. De Geer moraines and eskers in Pasvik, North Norway. In *Ten Years of Nordic Till Research*, Königsson LK (ed.). *Striae* **20**: 55–61.

Strömberg B. 1965. Mapping and geochronological investigations in some moraine areas of south-central Sweden. *Geografiska Annaler* **47A**: 73–82.

Strömberg B. 1981. Calving bays, striae and moraines at Gysinge-Hedesunda, central Sweden. *Geografiska Annaler* **63A**: 149–154.

Strömberg B. 1989. Late Weichselian deglaciation and clay varve chronology in east-central Sweden. Swedish Geological Survey, Ca 73; 70 pp.

Svedlund JO. 1991. Jordartkarta 25L Boden NO. Swedish Geological Survey, Ak 16.

Svedlund JO. 1992. Jordartkarta 25L Boden SO. Swedish Geological Survey, Ak 23.

Svendsen JI, Astakhov VI, Bolshiyanov DYu, Demidov I, Dowdeswell JA, Gataullin V, Hjort C, Hubberten HW, Larsen E, Mangerud J, Melles M, Möller P, Saarnisto M, Siegert MJ. 1999. Maximum extent of the Eurasian ice sheets in the Barents and Kara Sea region during the Weichselian. *Boreas* **28**: 234–242.

Thomas GSP, Connell RJ. 1985. Iceberg drop, dump and grounding structures from Pleistocene glacio-lacustrine sediments, Scotland. *Journal of Sedimentary Petrology* **55**: 243–249.

van der Veen CJ. 1996. Tidewater calving. *Journal of Glaciology* **42**: 375–385.

Walder JS, Fowler A. 1994. Channelized subglacial drainage over a deformable bed. *Journal of Glaciology* **40**: 199–200.

Warren CR. 1992. Iceberg calving and the glacioclimatic record. *Progress in Physical Geography* **16**: 253–282.

Warren CR, Glasser NF, Harrison S, Winchester V, Kerr AR, Rivera A. 1995. Characteristics of tide-water calving at Glaciar San Rafael, Chile. *Journal of Glaciology* **41**: 273–289.

Zilliacus H. 1985. On the moraine ridges east of Pohjankangas in northern Satakunta, western Finland. *Geologiska Föreningens i Stockholm Förhandlingar* **106**: 335–345.

Zilliacus H. 1987. De Geer moraines in Finland and the annual moraine problem. *Fennia* **165**: 147–239.

Zilliacus H. 1989. Genesis of De Geer moraines in Finland. *Sedimentary Geology* **62**: 309–317.